European Journal of Medicinal Chemistry 224 (2021) 113700

Contents lists available at ScienceDirect

European Journal of Medicinal Chemistry

journal homepage: http://www.elsevier.com/locate/ejmech

Discovery of novel trimethoxyphenylbenzo[*d*]oxazoles as dual tubulin/PDE4 inhibitors capable of inducing apoptosis at G2/M phase arrest in glioma and lung cancer cells

Jie liu [a, 1], Wan Ye [a, 1], Jiang-Ping Xu [a, d], Hai-Tao Wang [a], Xiao-Fang Li [c], Wen-Ya Wang [a, **], Zhong-Zhen Zhou [a, b, *]

[a] Guangdong Provincial Key Laboratory of New Drug Screening, School of Pharmaceutical Sciences, Southern Medical University, Guangzhou, 510515, China
[b] Pharmacy Department, Zhujiang Hospital, Southern Medical University, Guangzhou, 510515, China
[c] Department of Hematology, Nanfang Hospital, Southern Medical University, Guangzhou, 510515, PR China
[d] Key Laboratory of Mental Health of the Ministry Education, Southern Medical University, Guangzhou, 510515, China

ARTICLE INFO

Article history:
Received 18 April 2021
Received in revised form
9 June 2021
Accepted 10 July 2021
Available online 15 July 2021

Keywords:
Dual PDE4/Tubulin inhibitor
trimethoxyphenylbenzo[*d*]oxazole
Antiproliferative activities
Cell cycle arrest
Apoptosis

ABSTRACT

To discover PDE4/tubulin dual inhibitors with novel skeleton structures, 7-trimethoxyphenylbenzo[*d*]oxazoles **4a-u** and 4-trimethoxyphenylbenzo[*d*]oxazoles **5a-h** were designed and synthesized by migrating the trimethoxyphenyl group of TH03 to the benzo[*d*]oxazole moiety. Among these compounds, approximately half of them displayed good antiproliferative activities against glioma (U251) and lung cancer (A549 and H460) cell lines. The structure–activity relationships of trimethoxyphenylbenzo[*d*]oxazoles led to the identification of **4r** bearing indol-5-yl side-chain as a novel dual PDE4/tubulin inhibitor, which exhibited satisfactory antiproliferative activities against glioma (IC_{50} = 300 ± 50 nM) and lung cancer (average IC_{50} = 39.5 nM) cells. Further investigations revealed that **4r** induced apoptosis at G2/M phase arrest and disrupted the microtubule network. The preliminary mechanism of action showed that **4r** down-regulated the expression of cyclin B1 and its upstream regulator gene cdc25C in A549.

1. Introduction

Recent discoveries have indicated that single-target drugs are not sufficiently effective for the treatment of complex intractable diseases, such as neurological diseases [1] and cancer [2–5]. Since 2000, fast development of multitarget anticancer drugs was observed, and many multitarget anticancer drugs were approved owing to their satisfactory synergistic effects [6], such as entretinib (2019) [7], pyrotinib (2018) [8], duvelisib (2018) [9], and so on.

The proliferation and differentiation of tumor cells is a complex process, which involves several signaling molecules (e.g., cAMP and cGMP) and proteins (e.g., microtubule). Microtubules (MTs), such as α,β-tubulin heterodimers, play important roles in the mitosis and signaling molecules modulating apoptosis for the life cycle of the cell, and are important targets in cancer chemotherapy. Conversely, cyclic adenosine monophosphate (cAMP) is involved in various physiological processes, such as cell proliferation and differentiation, cell-cycle regulation, inflammation, and apoptosis, etc. [10,11]. PDE4, a cAMP-specific hydrolyzing enzyme, plays a significant role in asthma, chronic obstructive pulmonary disease (COPD), rheumatoid arthritis, Alzheimer's disease, depression, CNS tumors, and lung cancers [12–14]. And many PDE4 inhibitors [15–19] have been reported as therapeutics for the treatment of these diseases.

In addition, microtubule plays a vital role in the proliferation and differentiation of tumor cells, which leads it to one of the best targets for anti-cancer drugs. Anti-tubulin agents interfere in the dynamic polymerization and depolymerization process of microtubules. Unfortunately, these anti-tubulin agents are limited in the clinic for their toxicity effects and emergence of drug resistance [20]. One of the main reasons due to their non-selectivity toward the cancer cell line. Multitarget drugs incorporate the pharmacophores of two or more drugs into a single molecule, which interact

* Corresponding author. Guangdong Provincial Key Laboratory of New Drug Screening, School of Pharmaceutical Sciences, Southern Medical University, Guangzhou, 510515, China.
** Corresponding author.
E-mail addresses: wangwy@smu.edu.cn (W.-Y. Wang), zhouzz@smu.edu.cn (Z.-Z. Zhou).
[1] Both authors contributed equally to this work.

https://doi.org/10.1016/j.ejmech.2021.113700
0223-5234/

with multiple targets with minimal side effects [2,21]. PDE4/tubulin dual inhibitors were promoted in early 2012 [22], along with the discovery of 1, 1-diarylalkene derivatives (**1** and **2**) as PDE4 inhibitors capable of tubulin polymerization inhibitory activities. PDE4 is mainly expressed in the brain, liver, heart, lung, olfactory system, smooth muscle, endothelial cells, and immunocytes [13]. Therefore, we hypothesize that PDE4/tubulin dual inhibitors have selectivity toward the cancer cell line.

Our research group is devoted to discovering antitumor drugs with novel skeleton structures for the treatment of nervous system tumors and lung cancer, using PDE4 and tubulin as targets [23–26]. Recently, we discovered the trimethoxyphenylpyridine bearing 6-methoxybenzo[*d*]oxazole group (**TH03**, Fig. 1) [23] as a tubulin colchicine binding site inhibitor with potential anticancer activities toward human non-small cell lung cancer cells (A549) and glioma (U251) cells. In addition, some biphenyl derivatives demonstrated good inhibition activities against PDE4 [27–29]. Our previous studies described the discovery of the PDE4 inhibitor **BIPA29** with a biphenyl skeleton [29]. In this study, aiming to discover tubulin/PDE4 dual inhibitors with novel skeleton structures, trimethoxyphenylbenzo[*d*]oxazoles **4a**–**u** and **5a**–**h** were designed by migrating the trimethoxyphenyl group to benzo[*d*]oxazole. Their effects (*in vitro)* on lung cancer cell lines (A549 and H460), and glioma cell lines (U251), and their mechanisms of action therapy were elucidated.

2. Results and discussion

2.1. Chemistry

As described in Scheme 1, trimethoxyphenylbenzo[*d*]oxazoles **4a**–**u** and **5a**–**h** were synthesized in a two-step procedure, using 2-amino-phenols **6a**–**b** as starting material. Benzo[*d*]oxazole intermediates (**7a**–**v** and **8a**–**h**) were prepared via condensation of 2-amino-phenols **6a**–**b** with aryl chloride derivatives at 120 °C, or aryl aldehyde derivatives, followed by oxidation using 4-methoxy-TEMPO as oxygenant. Benzo[*d*]oxazoles **7n** and **7o** bearing hydroxyphenyl groups were obtained by the condensation reaction of **6b** and the corresponding aldehyde and directly used for the synthesis of the target compound without separation and purification. Benzo[*d*]oxazoles **7u** and **7v** bearing aminophenyl group were prepared by reduction of the corresponding **7p** and **7q** bearing nitrophenyl group. Subsequently, the target compounds **4a**–**u** and **5a**–**h** were obtained through the Suzuki reaction of 7-bromobenzo[*d*]oxazoles and 4-bromobenzo[*d*]oxazoles with trimethoxyphenylboronic acid respectively.

2.2. Pharmacological evaluation

2.2.1. Antiproliferative activities and SAR analysis

Antiproliferative activities of the target compounds **4a**–**u** and **5a**–**h** against a panel of human glioma (U251 cell lines), human lung cancer (A549 and H460 cell lines), and human breast cancer (MCF-7 cell lines) were evaluated using combretastatin A-4 (CA-4), colchicine (Col) and rolipram (Rol) as the positive control.

As shown in Table 1, trimethoxyphenylbenzo[*d*]oxazole derivatives **4a**–**u** and **5a**–**h** exhibited different activities against different types of tumors. Although trimethoxyphenylbenzo[*d*]oxazoles were inactive against MCF-7 cells, approximately half of trimethoxyphenylbenzo[*d*]oxazole derivatives displayed good antiproliferative activities against glioma (U251) cell lines and human lung cancer (A549 and H460) cell lines, ranging from 0.024 to 10 μM. Among these compounds, **4e**, **4h**, **4n**, **4p**, **4q,** and **4r** exhibited good activities against glioma and human lung cancer cells (0.024 < IC_{50} < 6.8 μM). Moreover, compound **4l** showed an IC_{50} value of 680 ± 80 nM against A549. More interesting, **4p** exhibited IC_{50} values of 720 nM (A549 cells) and 310 nM (H460 cells) against the tested human lung cancer. Furthermore, **4r** bearing 1*H*-indol-5-yl side-chain demonstrated the best antiproliferative activities (24 nM < IC_{50} < 300 nM) against glioma and

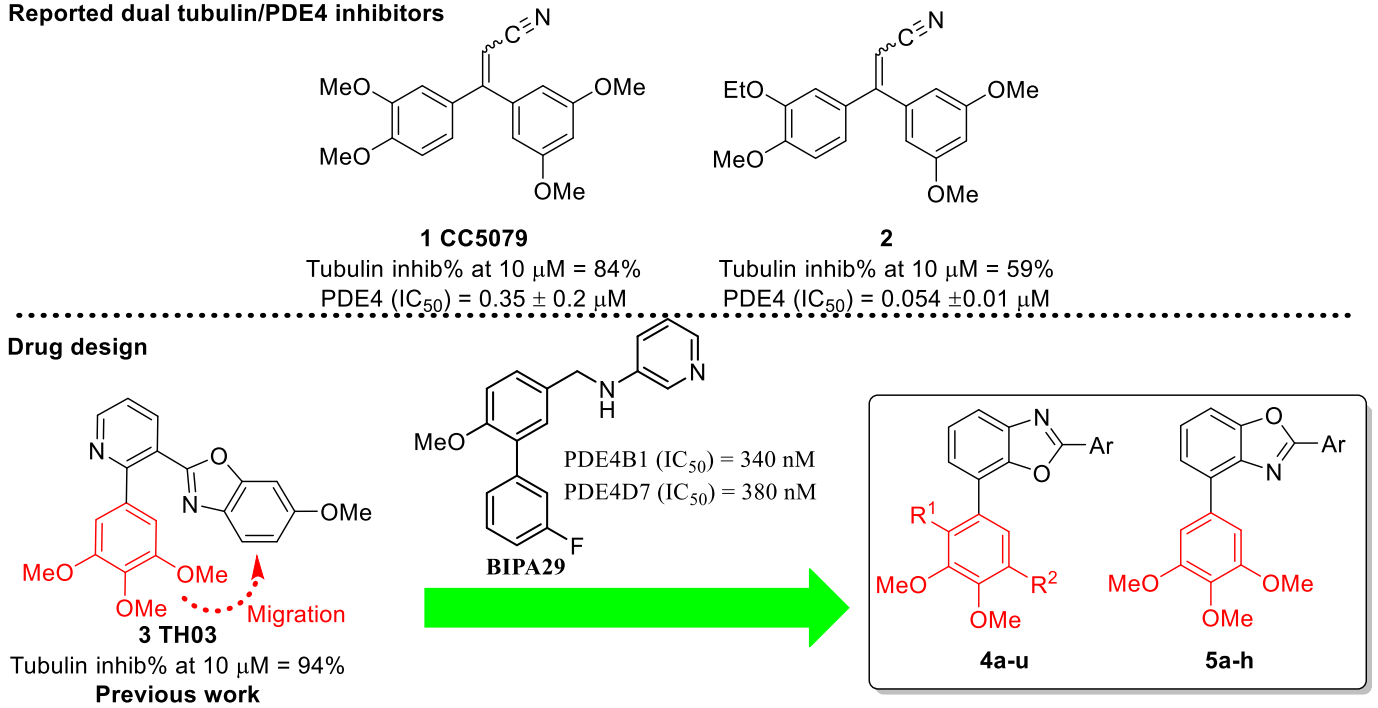

Fig. 1. Reported dual tubulin/PDE4 inhibitors and the proposed design of novel trimethoxyphenylbenzo[*d*] oxazoles.

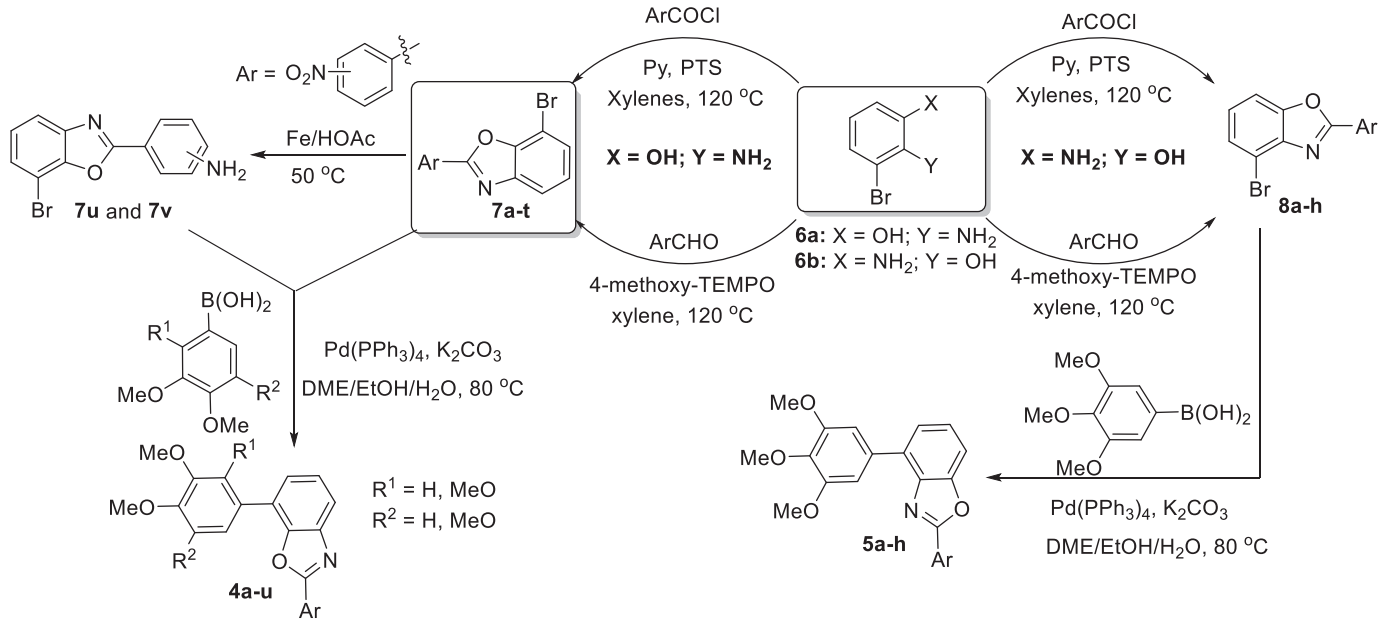

Scheme 1. Synthetic routes for trimethoxyphenylbenzo[*d*]oxazoles **4a**–**u** and **5a**–**h**.

human lung cancer cells. Compared to CA-4, **4r** was less effective against U251 cell lines, however, more active against human lung cancer cell lines with an IC_{50} value of 39.5 nM (the average of two human lung cancer cell lines).

Detailed analysis on the structure-activity relationships revealed that the position of the trimethoxyphenyl group on the benzo[*d*]oxazole has a great influence on antiproliferative activities. 7-trimethoxyphenylbenzo[*d*]oxazoles **4a**, **4d**–**g**, **4k,** and **4l** exhibited higher antiproliferative activities toward U251 and A549 cells compared with the corresponding 4-trimethoxyphenylbenzo[*d*] oxazoles **5a**–**h**. Moreover, the activity of **4r** bearing 3,4,5-trimethoxyphenyl group was higher than that of **4s** bearing 2,3,4-trimethoxyphenyl group. For 7-(3, 4, 5-trimethoxyphenyl) benzo [*d*]oxazoles **4a-r**, the substituents on the side-chain benzene ring significantly influenced their activities. For example, benzo[*d*]oxazole **4r** with an indole side-chain displayed higher antiproliferative activity than the corresponding benzo[*d*]oxazoles with mono-substituted phenyl side chains or disubstituted phenyl side chains.

2.2.2. Enzyme inhibition assay and immunofluorescence analysis

Base on the obtained antiproliferative activities, compounds **4l**, **4n, 4p, 4q, 4r**, **4t**, and **4u** were selected for the evaluation of the inhibition activities of microtubule assembly and PDE4 (Table 2), using combretastatin A-4 (CA-4), colchicine (Col), and rolipram (Rol) as the reference. As shown in Table 2, compound **4l** bearing 4-methyl phenyl side-chain exhibited good antiproliferative activities against A549 cells, but no inhibition activity toward tubulin polymerization and PDE4.

By replacing the 4-methyl phenyl side-chain of **4l** with hydrogen bond donor substituents on the side-chain benzene ring (i.e., **4n, 4p**, **4q,** and **4r)**, their tubulin polymerization inhibition activities increased. More interesting, replacing 4-methyl phenyl side-chain of **4l** with an indole side-chain, **4r** displayed higher tubulin polymerization inhibitory activities than colchicine at 10 μM. Additionally, **4r** demonstrated good PDE4 inhibition activity (IC_{50} = 1.25 μM), and nearly equal efficiency against tubulin polymerization. Based on these results, **4r** is a promising PDE4/tubulin inhibitor to treat lung cancer. Compared with tubulin inhibitor combretastatin A-4 (CA-4) and colchicine (Col), dual tubulin/PDE4 inhibitor **4r** showed a selectivity of tumor type. This may be due to the low expression of PDE4 in human breast [13]. So, dual tubulin/PDE4 inhibitor **4r** and PDE4 inhibitors (such as rolipram, **4t,** and **4u**) displayed no antiproliferative activities toward human breast cancer (MCF-7 cell lines). In addition, tubulin/PDE4 inhibitor **4r** showed more sensitive antiproliferative activity against lung cancer.

To further demonstrate the advantages of dual-target inhibitors, compounds **4t** and **4u** were designed and synthesized by replacing the indole side-chain with a five-membered heterocycle (such as thiophene ring or furan ring). Replacing the indole side-chain with furan ring **(4u),** the PDE4 inhibition activities were significantly increased. Compound **4u** bearing furan ring side-chain displayed good PDE4 inhibition activity (IC_{50} = 0.57 μM), which is higher than that of rolipram (Rol). Compared with PDE4 inhibitors (such as rolipram, **4t,** and **4u**), dual tubulin/PDE4 inhibitor **4r** demonstrated higher antiproliferative activities. These results suggested that dual tubulin/PDE4 inhibitors display good selectively and antiproliferative activities against lung cancer.

Tubulin plays a pivotal role in cell division owing to the dynamic polymerization and depolymerization process of the microtubules. Thus, the effects of **4r** on the cellular microtubule network were evaluated in A549 cells (Fig. 2). Compared to the 0.1% DMSO vehicle control group, the microtubule network (red) was disrupted by **4r** at the concentration of 50 and 500 nM, which is similar to that of CA-4. It revealed that **4r** strongly inhibited tubulin assembly in A549 cells.

2.2.3. Effect of 4r on the cell cycle and apoptosis

Several studies have confirmed that PDE4 inhibitors trigger apoptosis [13,25,30], while tubulin polymerization inhibitors arrest cells in the G2/M phase [31,32]. Therefore, the effects of **4r** on the cell cycles and cellular apoptosis in U251 and A549 cells were evaluated at different concentrations, using microtubular inhibitor combretastatin A-4 (CA-4) and PDE4 inhibitor rolipram as the reference.

As shown in Fig. 3, the G2/M arrest in A549 and U251 cell lines was induced by **4r** in a concentration-dependent manner after 24 h co-culture. The percentages of A549 and U251 cells at the G2/M

Table 1
Antiproliferative activities (IC_{50}, μM)[a] of trimethoxyphenylbenzo[*d*]oxazole derivatives **4a**–**u** and **5a**–**h**.

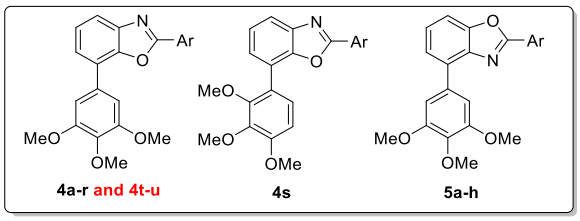

No.	Ar	Glioma	Lung cancer		Breast cancer
		U251	A549	H460	MCF-7
4a		3.5 ± 0.4	20.3 ± 2.6	6.8 ± 1.0	>25
4b		>25	2.2 ± 0.2	3.5 ± 0.6	>25
4c		>25	3.5 ± 0.4	>25	>25
4d		1.3 ± 0.1	2.8 ± 0.2	>25	>25
4e		1.7 ± 0.2	1.8 ± 0.2	2.8 ± 0.2	>25
4f		2.9 ± 0.1	2.6 ± 0.6	3.3 ± 0.6	>25
4g		>25	8.7 ± 0.5	8.7 ± 0.5	>25
4h		6.8 ± 0.3	2.1 ± 0.2	3.8 ± 0.5	>25
4i		>25	>25	>25	>25
4j		18.5 ± 2.0	>25	>25	>25
4k		1.6 ± 0.2	5.6 ± 0.8	>25	>25
4l		3.2 ± 0.3	0.68 ± 0.08	1.9 ± 0.7	>25
4m		>25	16.7 ± 0.8	>25	>25
4n		5.5 ± 0.1	2.0 ± 0.5	1.9 ± 0.2	>25
4o		10.3 ± 0.5	15.7 ± 0.4	2.0 ± 0 .1	>25
4p		1.04 ± 0.02	0.72 ± 0.09	0.31 ± 0.04	>25
4q		2.2 ± 0.1	4.7 ± 0.7	2.6 ± 0.4	>25
4r		0.30 ± 0.05	0.055 ± 0.006	0.024 ± 0.002	>25
4s		9.5 ± 1.3	9.6 ± 0.5	>25	>25
4t		10.6 ± 1.7	10.3 ± 1.5	2.6 ± 0.3	>25
4u		3.0 ± 0.2	12.5 ± 0.6	1.6 ± 0.02	>25

Table 1 (*continued*)

No.	Ar	Glioma	Lung cancer		Breast cancer
		U251	A549	H460	MCF-7
5a		>25	>25	9.0 ± 1.0	>25
5b		>25	20.1 ± 0.6	8.9 ± 1.0	>25
5c		>25	16.3 ± 1.7	5.7 ± 0.8	>25
5d		19.4 ± 1.4	>25	19.9 ± 0.7	>25
5e		>25	>25	>25	>25
5f		>25	>25	22.1 ± 1.7	>25
5g		>25	>25	8.6 ± 0.7	>25
5h		16.2 ± 0.3	20.2 ± 1.4	3.1 ± 0.3	>25
CA-4	-	0.13 ± 0.01	0.60 ± 0.12	0.076 ± 0.009	0.42 ± 0.13
Col	-	0.017 ± 0.001	0.024 ± 0.001	0.022 ± 0.001	0.040 ± 0.003
Rol	-	>100	>100	>100	>100

[a] All data were averaged over three separate experiments.

Table 2
Inhibitory activities of select compounds toward tubulin and PDE4.

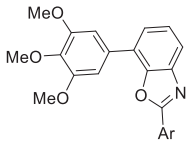

No.	Ar	Tubulin		PDE4CAT	
		1 μM (%)[a]	10 μM (%)[a]	1 μM (%)[a]	IC_{50} (μM)[a]
4l		NT[c]	18%	NA[b]	NT[c]
4n		5%	43%	NA[b]	NT[c]
4p		11%	36%	NA[b]	NT[c]
4q		14%	19%	NA[b]	NT[c]
4r		40%	86%	40%	1.25 ± 0.07
4t		NT[c]	0% (NA)	39%	3.3 ± 0.07
4u		NT[c]	0% (NA)	66%	0.57 ± 0.10
CA-4	-	52%	94%	-	-
Col	-	NT[c]	75%	-	-
Rol	-	-	-	59%	0.64 ± 0.09

[a] All data were averaged over three separate experiments.
[b] NA means "not active", which display the Inhibition rates (%) at 1 μM less than 10.0%.
[c] No tested.

phase increased to 68.09% (**4r** at 500 nM) and 71.69% (**4r** at 1000 nM), respectively. It has been reported that PDE4 inhibitor rolipram can block human hepatoma HepG2 cells in S phase at 10 μM [33], and arrest glioma cells in G0/G1 phase at 1 mM [34]. This suggests that PDE4 inhibitors have different cell-blocking abilities in different types of tumor cells. In A549 cells, **4r** induced the G2/M phase and S phase arrest, and the percentage of cells at the G0/G1 phases decreased simultaneously. Compared with CA-4, **4r** induced higher percentages of A549 at G2/M phase and S phase.

As shown in Fig. 4, PDE4 inhibitor rolipram induce weak apoptosis of A549 and U251 cells at low concentrations (200 nM and 500 nM), whereas microtubular inhibitor CA-4 induced obvious apoptosis of A549 and U251 cells. **4r** also induced obvious apoptosis of A549 and U251 cells after 24 h co-culture (Fig. 4). The percentages of apoptosis (early apoptotic cells and late apoptotic cells) by **4r** increased in a concentration-dependent manner, from 1.437% (A549 with 0.1% DMSO) and 2.39% (U251 with 0.1% DMSO) to 26.5% (A549 with **4r** at 500 nM) and 20.98% (U251 with **4r** at 1000 nM). Compared with CA-4, **4r** induced weak apoptosis in U251, but stronger apoptosis in A549.

According to these results, these results indicated that the dual tubulin/PDE4 inhibitor **4r** exhibited effects of PDE4 inhibitors and tubulin inhibitors on the cell cycles and apoptosis at the same time, which enhance its antitumor activities against human lung cancer cells. PDE4/tubulin inhibitor **4r** induced efficient G2/M and S phase arrest and apoptosis in A549 cells in a concentration-dependent manner, which stimulated further investigation on the cellular mechanisms of **4r**. It is well known that cyclin B1 and cdc25C play important roles in the regulation of G2/M conversion in the cell cycle. Overexpression of cyclin B1 can promote G2/M phase transformation, leading to uncontrolled cell proliferation and malignant transformation. The cdc2/cyclin B complex is a master switch for the G2/M phase transition to the G2 phase checkpoint during mitosis. When the phosphatase activity of cdc25C was inhibited, the complex activity is also blocked leading to mitosis arrest in the G2/M phase. As shown in Fig. 5, the expression of

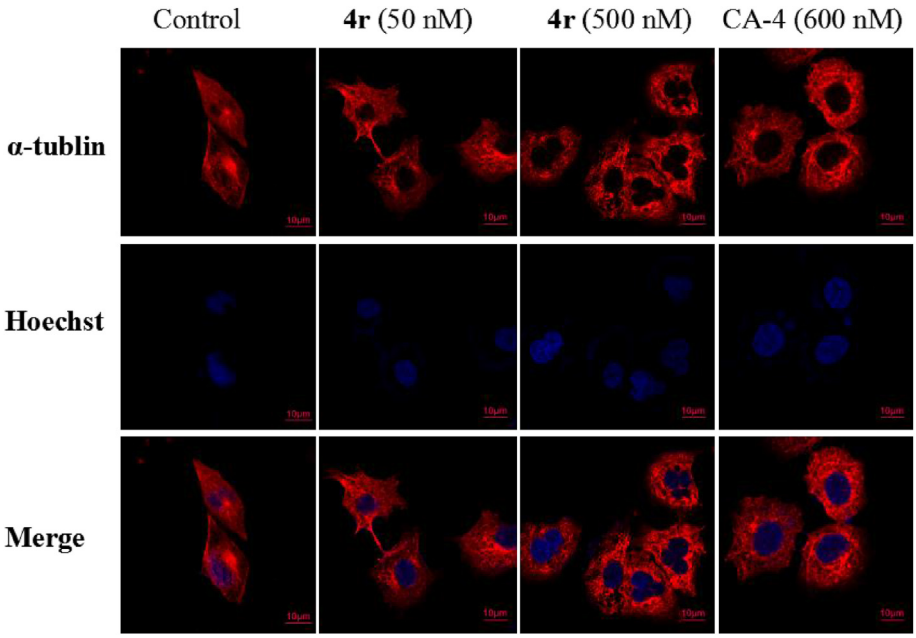

Fig. 2. Effects of **4r** on the A549 cellular microtubule network after 24h co-culture at the concentration of 50 nM and 500 nM, using CA-4 (600 nM) as positive control and DMSO (0.1% v/v) as vehicle control. Microtubules and the cell nucleus are stained in red and blue, respectively.

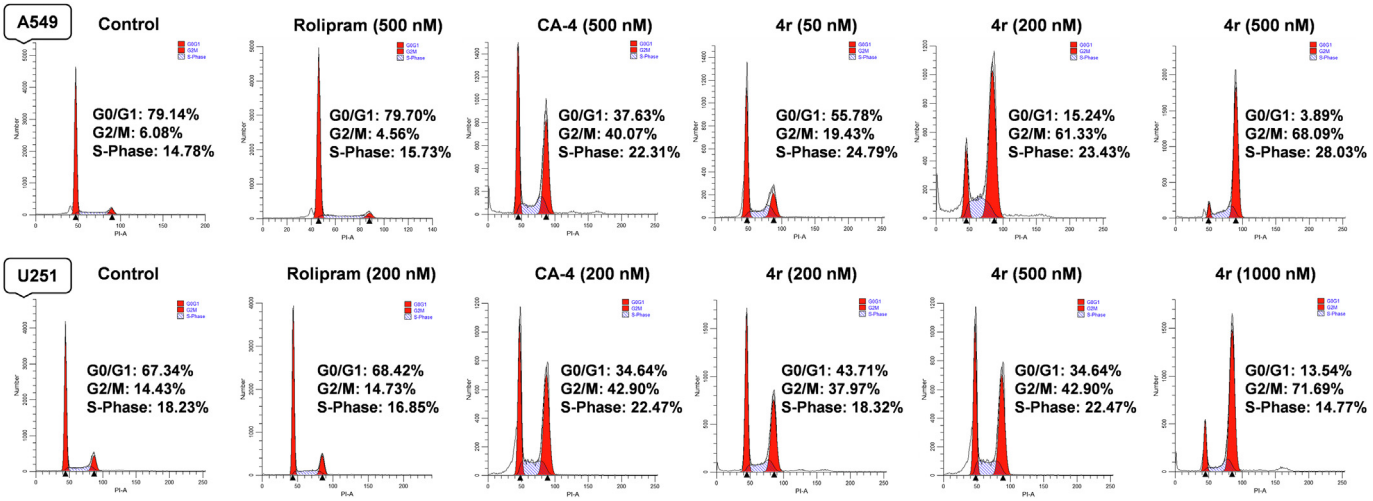

Fig. 3. Cell cycle analysis of **4r** on A549 and U251 cell lines at the different concentrations after 24 h co-culture, using DMSO (0.1% v/v) as vehicle control.

cyclin B1 and its upstream regulator gene cdc25C were down-regulated by **4r** in a dose-dependently manner.

2.3. Molecular docking

To further investigate structure-activity relationships, the molecular docking simulations of **4r** and **4s** in the active cavity of tubulin (PDB: 1SA0) [35]and PDE4 (PDB: 3G4L) [27] were performed in Maestro 11.1, using previously reported methods [23,29].

In the PDE4 active cavity (Fig. 6A), the 1*H*-Indolyl group forms one hydrogen bond (magenta dotted lines) with Val-238 residue, and a π−π interaction with Phe-538 residue. In addition, the benzo [*d*]oxazole ring forms two π−π interactions with Phe-538 and Phe-506 residues. 3,4,5-Trimethoxyphenyl group interacts with Asn375 residue through hydrogen bonds bridging with a water molecule. Replacing 3,4,5-trimethoxyphenyl group with 2,3,4-trimethoxyphenyl group, the interaction with Asn375 residue and π−π interactions with Phe-538 and Phe-506 residues were disappeared (Fig. 6C).

In the tubulin colchicine site (Fig. 6B), the binding poses of **4r** are similar to that of colchicine. The trimethoxyphenyl group in **4r** occupied the pocket of the trimethoxyphenyl group in the native ligand with some shifting. The slight shift resulted in two hydrogen bonds (magenta dotted lines) between the trimethoxyphenyl group and Cys-241 of the β-subunit. The NH moiety in the imidazole ring of 4r formed another hydrogen bond with the Ser-178 residue of the α-subunit. The glide docking scores for **4r** (−7.790) are higher than that of the native ligand (−6.853). Replacing 3,4,5-trimethoxyphenyl group with 2,3,4-trimethoxyphenyl group, the hydrogen bond between the Ser-178 residue and the imidazole ring of indole was disappeared. Molecular docking results showed that replacing 3,4,5-trimethoxyphenyl group with 2,3,4-

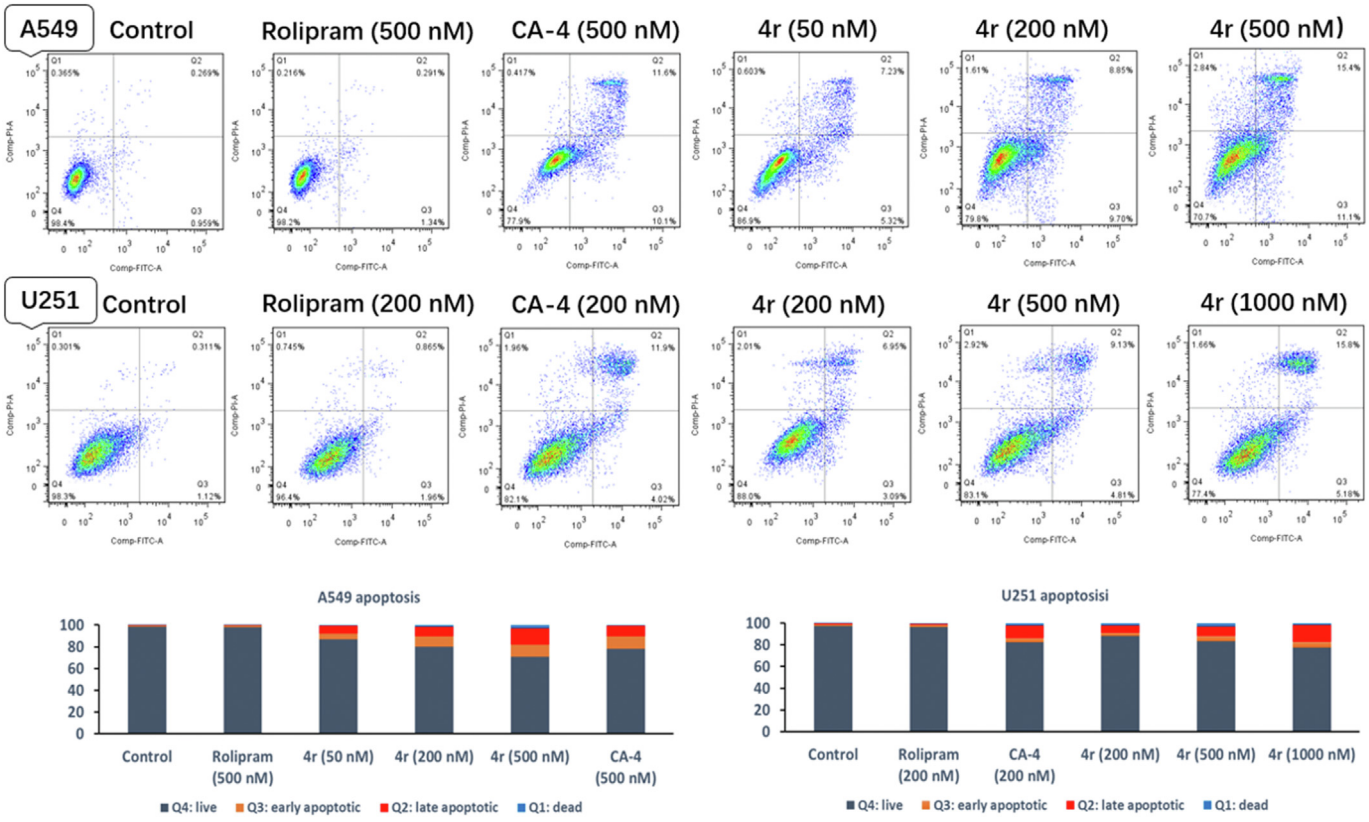

Fig. 4. Effect of **4r** on apoptosis after 24 h co-culture with A549 and U251 cell lines respectively, using DMSO (0.1% v/v) as vehicle control.

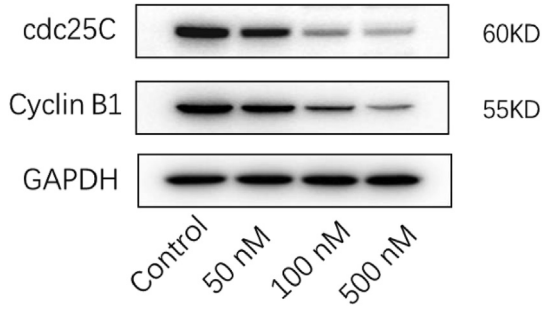

Fig. 5. Effect of **4r** on the expression of cyclin B1 and cdc25C in A549 cell lines at the different concentrations (50 nM, 100 nM, and 500 nM), using DMSO (0.1% v/v) as vehicle control.

trimethoxyphenyl group was detrimental to its inhibitory activities toward PDE4 and tubulin, which are in good agreement with structure-activity relationships.

3. Conclusion

In this study, a series of novel trimethoxyphenylbenzo[d]oxazoles was synthesized and screened for their antitumor activities. The screening results of antiproliferation inhibitory activity revealed that trimethoxyphenylbenzo[*d*]oxazole derivatives were inactive against MCF-7 cells; however, good antiproliferative activities against glioma (U251) cell lines and human lung cancer (A549 and H460) cell lines were observed. The SAR analysis of these compounds revealed that the **4r** bearing an indole side-chain as PDE4/tubulin inhibitor exhibited the best antiproliferative activities (24 nM < IC_{50} < 300 nM) against glioma and human lung cancer cells. Further investigations revealed that **4r** arrests the cell cycle in the G2/M phase by down-regulating the expression of cyclin B1 and its upstream regulator gene cdc25C, disrupting the microtubules network, and consequently inducing efficient apoptosis.

4. Experimental section

4.1. Chemistry with materials and methods

All purchased reagents and solvents were used without further purification. The products were purified using a preparative chromatography (Isolera™ Prime) or TLC (thin-layer chromatography) silica gel plate with the solvent system indicated, or by column chromatography on silica gel (200–300 mesh). NMR spectra were recorded on Varian Mercury 400 spectrometer with $CDCl_3$ or DMSO-d_6 solution. LC-MS spectra data were obtained by a Waters UPLC/Quattro Premier XE mass spectrometer. High-resolution mass spectrometry (HRLC-MS) data were acquired by Thermo Scientific Orbitrap Fusion Tribrid mass spectrometer. Melting points were determined in open glass capillaries by an uncorrected X-5 apparatus.

4.1.1. General procedures for the synthesis of bromobenzo[d]oxazole analogs

General procedure A: Aryl chloride (1 mmol) and pyridine (81 μL) were added sequentially to a solution of 2-amino-6-bromophenol (1 mmol, 188 mg) in xylene (3.5 mL) at room temperature. The mixture was stirred for 1 h at room temperature. Then, *p*-toluenesulfonic acid (3 mmol) was added to the mixture. The reaction mixture was stirred at 120 °C for 18 h, and monitored by thin-layer chromatography. After the reaction was completed, the reaction mixture was cooled to room temperature, dumped into

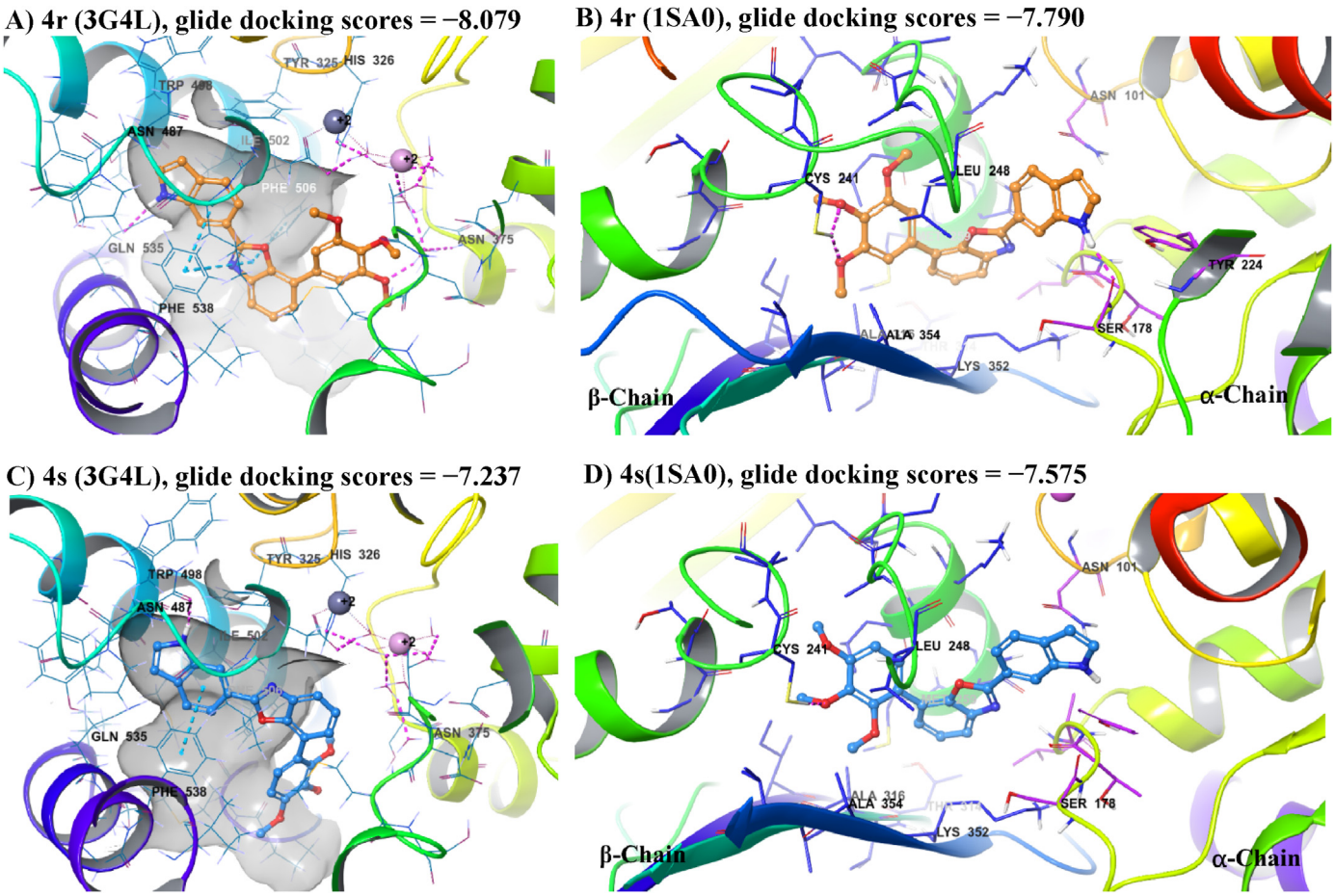

Fig. 6. Proposed binding models of **4r (**the orange ball and stick model**)** and **4s** (the azure ball and stick model) with PDE4 (A, PDB 3G4L) and tubulin (B, PDB: 1SA0). The glide docking scores of the native ligand roflumilast and DAMA−colchicine (green stick model) are −9.078 (3G4L) and −6.853 (1SA0), respectively.

the water (50 mL), and extracted using ethyl acetate (2 × 20 mL). The combined organic phases were dried with anhydrous sodium sulfate. After filtration and evaporation, the pure product was obtained by chromatography (n-hexane: ethyl acetate = 25: 1, v\v).

General procedure B: 2-amino-6-bromophenol (1 mmol, 188 mg) and the corresponding aldehyde were deposited inside a sealed pressure tube. The tube was vacuumed using an oil pump, and then gently flushed with an ordinary purity oxygen balloon. After exchanging oxygen and air three times, xylene (5 mL) was added. Then, the mixture was stirred at room temperature. After dissolving the solids, the reaction mixture was stirred at 120 °C. After 0.5 h, a solution of xylene (0.3 mL) containing 4-methoxy-TEMPO (0.05 mmol, 9.3 mg) was added to the mixture, which was then stirred at 120 °C for 5 h, and monitored by thin-layer chromatography. After the reaction was completed, the reaction mixture was cooled to room temperature, and concentrated under reduced pressure. The purified compound was obtained by column chromatography (n-hexane: ethyl acetate = 15:1, v\v) of the acquired residue from the previous step.

General procedure C: Reduced iron powder (5 mmol, 280 mg) was added to a solution of bromobenzo[***d***]oxazole bearing nitrophenyl group (1 mmol) in a mixture of solvents (methanol\acetic acid = 1\1, 3 mL). Then, the mixture was stirred at 50 °C for 3 h under an argon atmosphere, and monitored by thin-layer chromatography. After the reaction was completed, the reaction mixture was cooled to room temperature and filtered. The solvent in the obtained filtrate was removed under reduced pressure to give the crude residue, which was then purified by column chromatography (n-hexane: ethyl acetate = 10:1, v\v) to provide the product.

7-Bromo-2-phenylbenzo[*d*]oxazole (7a). According to the procedure A, **7a** was synthesized by intermolecular condensation reaction of 2-amino-6-bromophenol (1 mmol, 188 mg) and benzoyl chloride (1 mmol, 140 mg) as a white powdery solid (isolated yield = 85%). M.p.: 82.5−84.4 °C. ^{1}H NMR (400 MHz, $CDCl_3$) δ 8.29−8.27 (m, 2H), 7.70 (d, *J* = 7.8 Hz, 1H), 7.58−7.52 (m, 3H), 7.49 (d, *J* = 7.4 Hz, 1H), 7.24 (t, *J* = 8.0 Hz, 1H). ^{13}C NMR (101 MHz, $CDCl_3$) δ 163.20, 148.97, 142.83, 131.95, 128.96, 128.19, 127.86, 126.56, 125.73, 119.03, 102.52.

7-Bromo-2-(4-methoxyphenyl)benzo[*d*]oxazole (7b). According to the procedure A, **7b** was synthesized by intermolecular condensation reaction of 2-amino-6-bromophenol (1 mmol, 188 mg) and 4-methoxybenzoyl chloride (1 mmol, 170 mg) as a light pink solid (isolated yield = 82%). M.p.:128.9−129.9 °C. ^{1}H NMR (400 MHz, $CDCl_3$) δ 8.22 (d, *J* = 8.8 Hz, 2H), 7.65 (dd, *J* = 8.0, 0.4 Hz, 1H), 7.45 (dd, *J* = 8.0, 0.4 Hz, 1H), 7.21 (t, *J* = 10.6 Hz, 1H), 7.03 (d, *J* = 8.8 Hz, 2H), 3.90 (s, 3H). ^{13}C NMR (101 MHz, $CDCl_3$) δ 163.34, 162.68, 148.86, 143.04, 129.68, 127.68, 125.58, 119.04, 118.62, 114.42, 102.32, 55.47.

7-Bromo-2-(3-methoxyphenyl)benzo[*d*]oxazole (7c). According to the procedure A, **7c** was synthesized by intermolecular condensation reaction of 2-amino-6-bromophenol (1 mmol, 188 mg) and 3-methoxybenzoyl chloride (1 mmol, 170 mg) as a white solid (isolated yield = 64%). M.p.:102.4−103.8 °C. ^{1}H NMR

(400 MHz, $CDCl_3$) δ 7.86 (d, J = 7.8 Hz, 1H), 7.77 (s, 1H), 7.68 (dd, J = 8.0, 0.6 Hz, 1H), 7.47 (dd, J = 8.0, 0.6 Hz, 1H), 7.42 (t, J = 8.0 Hz, 1H), 7.22 (t, J = 8.0 Hz, 1H), 7.08 (dd, J = 8.4, 1.6 Hz, 1H), 3.91 (s, 3H). ^{13}C NMR (101 MHz, $CDCl_3$) δ 163.03, 159.88, 148.88, 142.71, 130.01, 128.19, 127.63, 125.69, 120.31, 118.97, 118.55, 112.16, 102.49, 55.49.

7-Bromo-2-(3,4-dimethoxyphenyl)benzo[*d*]oxazole (7d). According to the procedure A, **7d** was synthesized by intermolecular condensation reaction of 2-amino-6-bromophenol (1 mmol, 188 mg) and 3,4-dimethoxybenzoyl chloride (1 mmol, 200 mg) as a white solid (isolated yield = 61%). M.p.: 158.4–159.5 °C. ^{1}H NMR (400 MHz, $CDCl_3$) δ 7.68 (d, J = 8.0 Hz, 1H), 7.48 (d, J = 8.0 Hz, 1H), 7.40 (d, J = 2.0 Hz, 2H), 7.22 (t, J = 8.0 Hz, 1H), 6.63 (t, J = 2.0 Hz, 1H), 3.89 (s, 6H). ^{13}C NMR (101 MHz, $CDCl_3$) δ 163.03, 161.08, 148.89, 142.68, 128.27, 128.08, 125.71, 118.98, 105.51, 104.79, 102.51, 55.64.

7-Bromo-2-(3-fluoro-4-methoxyphenyl)benzo[*d*]oxazole (7e). According to the procedure A, **7e** was synthesized by intermolecular condensation reaction of 2-amino-6-bromophenol (1 mmol, 188 mg) and 3-fluoro-4-methoxybenzoyl chloride (1 mmol, 188 mg) as a white solid (isolated yield = 65%). M. p.: 179.5–180.9 °C. ^{1}H NMR (400 MHz, $CDCl_3$) δ 8.03 (d, J = 8.8 Hz, 1H), 7.99 (d, J = 11.6 Hz, 1H), 7.66 (d, J = 8.0 Hz, 1H), 7.47 (d, J = 8.0 Hz, 1H), 7.22 (t, J = 8.0 Hz, 1H), 7.08 (t, J = 8.4 Hz, 1H), 3.98 (s, 3H). ^{13}C NMR (101 MHz, $CDCl_3$) δ 162.15 (d, J = 3.0 Hz), 152.25 (d, J = 249 Hz), 150.96 (d, J = 14 Hz), 148.90, 142.84, 128.05, 125.76, 124.63 (d, J = 4.0 Hz), 119.37 (d, J = 7.0 Hz), 118.82, 115.56 (d, J = 20 Hz), 113.26 (d, J = 2.0 Hz), 102.40, 56.31.

7-Bromo-2-(3-fluorophenyl)benzo[*d*]oxazole (7f). According to the procedure A, **7f** was synthesized by intermolecular condensation reaction of 2-amino-6-bromophenol (1 mmol, 188 mg) and 3-fluorobenzoyl chloride (1 mmol, 158.5 mg) as a white solid (isolated yield = 69%). M. p.: 116.2–117.3 °C. ^{1}H NMR (400 MHz, $CDCl_3$) δ 8.05 (d, J = 7.8 Hz, 1H), 7.96–7.93 (m, 1H), 7.69 (d, J = 7.8 Hz, 1H), 7.52–7.47 (m, 2H), 7.26–7.21 (m, 2H). ^{13}C NMR (101 MHz, $CDCl_3$) δ 162.86 (d, J = 246 Hz), 161.87 (d, J = 4.0 Hz), 148.94, 142.60, 130.68 (d, J = 8.0 Hz), 128.56, 128.52 (d, J = 8.0 Hz), 125.90, 123.54 (d, J = 3.0 Hz), 119.21, 118.94 (d, J = 21 Hz), 114.74 (d, J = 24 Hz), 102.59.

7-Bromo-2-(4-fluorophenyl)benzo[*d*]oxazole (7g). According to the procedure A, **7g** was synthesized by intermolecular condensation reaction of 2-amino-6-bromophenol (1 mmol, 188 mg) and 4-fluorobenzoyl chloride (1 mmol, 158.5 mg) as a white solid (isolated yield = 64%). M. p.: 156.2–158.1 °C. ^{1}H NMR (400 MHz, $CDCl_3$) δ 8.29 (d, J = 5.6 Hz, 1H), 8.27 (d, J = 5.6 Hz, 1H), 7.68 (d, J = 7.4 Hz, 1H), 7.48 (d, J = 8.0 Hz, 1H), 7.25–7.20 (m, 3H). ^{13}C NMR (101 MHz, $CDCl_3$) δ 165.06 (d, J = 252 Hz), 162.27, 148.96, 142.76, 130.13 (d, J = 9.0 Hz), 128.22, 125.81, 122.87 (d, J = 3.0 Hz), 118.99, 116.28 (d, J = 22 Hz), 102.49.

7-Bromo-2-(3-bromophenyl)benzo[*d*]oxazole (7h). According to the procedure A, **7h** was synthesized by intermolecular condensation reaction of 2-amino-6-bromophenol (1 mmol, 188 mg) and 3-bromobenzoyl chloride (1 mmol, 219.5 mg) as a white solid (isolated yield = 62%). M. p.: 137.4–138.5 °C. ^{1}H NMR (400 MHz, $CDCl_3$) δ 8.41 (t, J = 1.6 Hz, 1H), 8.19 (dd, J = 7.8, 1.0 Hz, 1H), 7.70–7.66 (m, 2H), 7.50 (d, J = 8.0 Hz, 1H), 7.40 (t, J = 8.0 Hz, 1H), 7.24 (t, J = 8.0 Hz, 1H). ^{13}C NMR (101 MHz, $CDCl_3$) δ 161.57, 148.96, 142.56, 134.82, 130.62, 130.47, 128.60, 128.40, 126.29, 125.94, 123.04, 119.22, 102.61.

7-Bromo-2-(4-bromophenyl)benzo[*d*]oxazole (7i). According to the procedure A, **7i** was synthesized by intermolecular condensation reaction of 2-amino-6-bromophenol (1 mmol, 188 mg) and 4-bromobenzoyl chloride (1 mmol, 219.5 mg) as a white solid (isolated yield = 75%). M.p.:170.9–172.0 °C. ^{1}H NMR (400 MHz, $CDCl_3$) δ 8.15 (d, J = 8.6 Hz, 2H), 7.71–7.67 (m, 3H), 7.51 (dd, J = 8.0, 0.8 Hz, 1H), 7.25 (t, J = 8.0 Hz, 1H). ^{13}C NMR (101 MHz, $CDCl_3$) δ 162.31, 148.97, 142.72, 132.33, 129.23, 128.48, 126.79, 125.93, 125.49, 119.13, 102.58.

7-Bromo-2-(3-chlorophenyl)benzo[*d*]oxazole (7j) According to the procedure A, **7j** was synthesized by intermolecular condensation reaction of 2-amino-6-bromophenol (1 mmol, 188 mg) and 3-chlorobenzoyl chloride (1 mmol, 175 mg) as a white solid (isolated yield = 75%). M. p.: 158.1–159.0 °C. ^{1}H NMR (400 MHz, $CDCl_3$) δ 8.21 (d, J = 8.4 Hz, 2H), 7.69 (d, J = 8.0 Hz, 1H), 7.52–7.49 (m, 3H), 7.24 (t, J = 7.6 Hz, 1H). ^{13}C NMR (101 MHz, $CDCl_3$) δ 162.20, 148.95, 142.71, 138.28, 129.34, 129.07, 128.43, 125.89, 125.03, 119.10, 102.55.

7-Bromo-2-(4-chlorophenyl)benzo[*d*]oxazole (7k). According to the procedure A, **7k** was synthesized by intermolecular condensation reaction of 2-amino-6-bromophenol (1 mmol, 188 mg) and 4-chlorobenzoyl chloride (1 mmol, 175 mg) as a white solid (isolated yield = 73%). M. p.: 137.4–138.5 °C. ^{1}H NMR (400 MHz, $CDCl_3$) δ 8.21 (d, J = 8.6 Hz, 2H), 7.69 (d, J = 8.0 Hz, 1H), 7.53–7.49 (m, 3H), 7.24 (t, J = 8.0 Hz, 1H). ^{13}C NMR (101 MHz, $CDCl_3$) δ 162.21, 148.96, 142.72, 138.29, 129.35, 129.08, 128.43, 125.90, 125.04, 119.11, 102.56.

7-Bromo-2-(*p*-tolyl)benzo[*d*]oxazole (7l). According to the procedure A, **7l** was synthesized by intermolecular condensation reaction of 2-amino-6-bromophenol (1 mmol, 188 mg) and 4-methylbenzoyl chloride (1 mmol, 154 mg) as a white solid (isolated yield = 84%). M.p.: 97.5–98.7 °C. ^{1}H NMR (400 MHz, $CDCl_3$) δ 8.17 (d, J = 8.0 Hz, 2H), 7.68 (d, J = 8.0 Hz, 1H), 7.47 (d, J = 8.0 Hz, 1H), 7.34 (d, J = 8.0 Hz, 2H), 7.23 (t, J = 8.0 Hz, 1H), 2.45 (s, 3H). ^{13}C NMR (101 MHz, $CDCl_3$) δ 163.46, 148.88, 142.91, 142.59, 129.69, 127.95, 127.82, 125.63, 123.77, 118.84, 102.43, 21.68.

7-Bromo-2-(*m*-tolyl)benzo[*d*]oxazole (7m). According to the procedure A, **7m** was synthesized by intermolecular condensation reaction of 2-amino-6-bromophenol (1 mmol, 188 mg) and 3-methylbenzoyl chloride (1 mmol, 154 mg) as a white solid (isolated yield = 57%). M.p.:100.5–102.2 °C. ^{1}H NMR (400 MHz, $CDCl_3$) δ 8.10–8.07 (m, 2H), 7.69 (d, J = 8.0 Hz, 1H), 7.48 (d, J = 8.0 Hz, 1H), 7.42 (t, J = 7.4 Hz, 1H), 7.37 (d, J = 7.4 Hz, 1H), 7.23 (t, J = 8.0 Hz, 1H), 2.46 (s, 3H). ^{13}C NMR (101 MHz, $CDCl_3$) δ 163.41, 148.94, 142.83, 138.82, 132.80, 128.86, 128.34, 128.11, 126.40, 125.69, 125.04, 118.96, 102.49, 21.33.

7-Bromo-2-(4-nitrophenyl)benzo[*d*]oxazole (7p). According to the procedure B, **7p** was synthesized by intermolecular condensation reaction of 2-amino-6-bromophenol (1 mmol, 188 mg) and *p*-nitrobenzaldehyde (1 mmol, 151 mg) as a white powder (isolated yield = 89%). M. p.: 184.2–185.3 °C. ^{1}H NMR (400 MHz, DMSO-d_6) δ 8.48–8.43 (m, 4H), 7.91 (d, J = 8.0 Hz, 1H), 7.74 (d, J = 8.0 Hz, 1H), 7.43 (t, J = 8.0 Hz, 1H). ^{13}C NMR (101 MHz, DMSO-d_6) δ 160.78, 149.56, 148.76, 142.32, 131.61, 129.47, 129.00, 127.11, 124.76, 120.07, 102.26.

7-bromo-2-(3-nitrophenyl)benzo[*d*]oxazole (7q): According to the procedure B, **7q** was synthesized by intermolecular condensation reaction of 2-amino-6-bromophenol (1 mmol, 188 mg) and 3-nitrobenzaldehyde (1 mmol, 151 mg) as a light gray powder (isolated yield = 83%). M. p.: 152.3–153.9 °C. ^{1}H NMR (400 MHz, DMSO-d_6) δ 8.84 (s, 1H), 8.60 (d, J = 8.0 Hz, 1H), 8.50 (dd, J = 8.4, 1.4 Hz, 1H), 7.94 (t, J = 8.0 Hz, 1H), 7.89 (d, J = 8.0 Hz, 1H), 7.73 (d, J = 8.0 Hz, 1H), 7.42 (t, J = 8.0 Hz, 1H). ^{13}C NMR (101 MHz, DMSO-d_6) δ 160.61, 148.57, 148.40, 142.14, 133.52, 131.50, 129.18, 127.49, 126.98, 126.76, 121.92, 119.85, 102.18.

7-Bromo-2-(1*H*-indol-5-yl)benzo[*d*]oxazole (7r). According to the procedure B, **7r** was synthesized by intermolecular condensation reaction of 2-amino-6-bromophenol (1 mmol, 188 mg) and 1*H*-indole-5-carbaldehyde (1 mmol, 145 mg) as a white solid (isolated yield = 97%). M. p.: 137.8–138.6 °C. ^{1}H NMR (400 MHz, DMSO-d_6) δ 11.56 (s, 1H), 8.48 (s, 1H), 7.97 (dd, J = 8.6, 1.6 Hz, 1H), 7.77 (d, J = 8.0 Hz, 1H), 7.63 (d, J = 8.6 Hz, 1H), 7.59 (d, J = 8.0 Hz, 1H), 7.53 (t, J = 2.8 Hz, 1H), 7.34 (t, J = 8.0 Hz, 1H), 6.69 (s, 1H). ^{13}C NMR (101 MHz, DMSO-d_6) δ 164.51, 148.32, 142.96, 138.20, 127.99, 127.63,

127.55, 126.31, 120.78, 120.59, 118.80, 116.66, 112.56, 102.75, 101.65.

7-Bromo-2-(furan-2-yl)benzo[d]oxazole (7s). According to the procedure A, **7s** was synthesized by intermolecular condensation reaction of 2-amino-6-bromophenol (1 mmol, 188 mg) and furan-2-carbonyl chloride (1 mmol, 131 mg) as a yellow powdery solid (isolated yield = 65%). M. p.: 135.6–136.1 °C. ^{1}H NMR (400 MHz, $CDCl_3$) δ 7.69–7.66 (m, 2H), 7.48 (d, *J* = 8.0 Hz, 1H), 7.34 (d, *J* = 3.6 Hz, 1H), 7.23 (t, *J* = 8.0 Hz, 1H), 6.63 (dd, *J* = 3.4, 1.6 Hz, 1H). ^{13}C NMR (101 MHz, CDCl3) δ 155.26, 148.31, 146.15, 142.35, 141.94, 128.30, 125.95, 119.07, 115.17, 112.31, 102.38.

7-Bromo-2-(thiophen-2-yl)benzo[d]oxazole (7t). According to the procedure A, **7t** was synthesized by intermolecular condensation reaction of 2-amino-6-bromophenol (1 mmol, 188 mg) and thiophene-2-carbonyl chloride (1 mmol, 147 mg) as a light pink solid (isolated yield = 53%). M. p.: 117.4–119.3 °C. ^{1}H NMR (400 MHz, $CDCl_3$) δ 7.99–7.97 (m, 1H), 7.65 (d, *J* = 8.0 Hz, 1H), 7.59 (d, *J* = 5.0 Hz, 1H), 7.47 (d, *J* = 8.0 HZ, 1H), 7.24–7.17 (m, 2H). ^{13}C NMR (101 MHz, $CDCl_3$) δ 148.63, 142.73, 130.93, 130.74, 128.88, 128.33, 128.15, 125.87, 118.78, 102.30.

4-(7-Bromobenzo[*d*]oxazol-2-yl)aniline (7u). According to the procedure C, **7s** was synthesized by reduction of 7p (1 mmol, 319 mg) as a light gray powder product (isolated yield = 96%). M. p.: 175.4–177.1 °C. ^{1}H NMR (400 MHz, DMSO-d_6) δ 7.88 (d, *J* = 8.6 Hz, 2H), 7.66 (d, *J* = 7.8 Hz, 1H), 7.51 (d, *J* = 8.0 Hz, 1H), 7.28 (t, *J* = 8.0 Hz, 1H), 6.73 (d, *J* = 8.6 Hz, 2H), 6.09 (s, 2H). ^{13}C NMR (101 MHz, DMSO-d_6) δ 163.97, 153.15, 148.02, 143.16, 129.40, 126.93, 126.11, 118.28, 113.75, 112.01, 101.39.

3-(7-Bromobenzo[*d*]oxazol-2-yl)aniline (7v). According to the procedure C, **7t** was synthesized by reduction of 7q (1 mmol, 319 mg) as a white solid (isolated yield = 95%). M. p.: 157.9–158.4 °C. ^{1}H NMR (400 MHz, DMSO-d_6) δ 7.79 (d, *J* = 7.8 Hz, 1H), 7.64 (d, *J* = 7.8 Hz, 1H), 7.44 (s, 1H), 7.38–7.35 (m, 2H), 7.26 (t, *J* = 7.8 Hz, 1H), 6.83 (d, *J* = 7.6 Hz, 1H), 5.55 (s, 2H). ^{13}C NMR (101 MHz, DMSO-d_6) δ 163.45, 149.70, 148.34, 142.58, 130.08, 128.26, 126.56, 126.44, 119.33, 117.92, 115.02, 112.22, 101.88.

4-Bromo-2-phenylbenzo[*d*]oxazole (8a). According to the procedure A, **8a** was synthesized by intermolecular condensation reaction of 2-amino-3-bromophenol (1 mmol, 188 mg) and benzoyl chloride (1 mmol, 140.5 mg) as a white solid (isolated yield = 85%). M. p.: 112.4–114.6 °C. ^{1}H NMR (400 MHz, $CDCl_3$) δ 8.30 (dd, *J* = 8.0, 1.4 Hz, 2H), 7.57–7.50 (m, 5H), 7.22 (t, *J* = 8.0 Hz, 1H). ^{13}C NMR (101 MHz, $CDCl_3$) δ 163.49, 150.82, 141.67, 131.93, 128.86, 127.97, 127.78, 126.57, 125.87, 112.70, 109.72.

4-Bromo-2-(3,4-dimethoxyphenyl)benzo[*d*]oxazole (8b). According to the procedure A, **8b** was synthesized by intermolecular condensation reaction of 2-amino-3-bromophenol (1 mmol, 188 mg) and 3,4-dimethoxybenzoyl chloride (1 mmol, 200 mg) as a white solid (isolated yield = 64%). M. p.: 147.1–148.9 °C. ^{1}H NMR (400 MHz, $CDCl_3$) δ 7.90 (dd, *J* = 8.4,1.8 Hz, 1H), 7.80 (d, *J* = 1.8 Hz, 1H), 7.51 (d, *J* = 8.0 Hz, 2H), 7.20 (t, *J* = 8.0 Hz, 1H), 6.99 (d, *J* = 8.4 Hz, 1H), 4.03 (s, 3H), 3.98 (s, 3H). ^{13}C NMR (101 MHz, $CDCl_3$) δ 163.60, 152.35, 150.76, 149.20, 141.82, 127.66, 125.44, 121.72, 119.17, 112.24, 110.96, 110.43, 109.49, 56.20, 56.04.

4-Bromo-2-(3,5-dimethoxyphenyl)benzo[*d*]oxazole (8c). According to the procedure A, **8c** was synthesized by intermolecular condensation reaction of 2-amino-3-bromophenol (1 mmol, 188 mg) and 3,5-dimethoxybenzoyl chloride (1 mmol, 200 mg) as a white solid (isolated yield = 69%). M. p.: 154.3–155.2 °C. ^{1}H NMR (400 MHz, $CDCl_3$) δ 7.53 (d, *J* = 8.0 Hz, 2H), 7.44 (s, 2H), 7.23 (t, *J* = 8.0 Hz, 1H), 6.64 (s, 1H), 3.90 (s, 6H). ^{13}C NMR (101 MHz, $CDCl_3$) δ 163.38, 161.06, 150.79, 141.59, 128.17, 127.83, 125.98, 112.69, 109.74, 105.63, 104.98, 55.70.

4-Bromo-2-(3-fluoro-4-methoxyphenyl)benzo[*d*]oxazole (8d). According to the procedure A, **8d** was synthesized by intermolecular condensation reaction of 2-amino-3-bromophenol (1 mmol, 188 mg) and 3-fluoro-4-methoxybenzoyl chloride (1 mmol, 188 mg) as a white solid (isolated yield = 71%). M. p.: 124.3–125.1 °C. ^{1}H NMR (400 MHz, $CDCl_3$) δ 8.06 (d, *J* = 8.8 Hz, 1H), 8.01 (dd, *J* = 11.6, 2.0 Hz, 1H), 7.52 (d, *J* = 3.6 Hz, 1H), 7.50 (d, *J* = 3.6 Hz, 1H), 7.21 (t, *J* = 8.0 Hz, 1H), 7.08 (t, *J* = 8.4 Hz, 1H), 3.98 (s, 3H). ^{13}C NMR (101 MHz, $CDCl_3$) δ 162.45 (d, *J* = 3.0 Hz), 152.14 (d, *J* = 256 Hz), 150.96, 150.74,141.66, 127.78, 125.72, 124.76 (d, *J* = 4.0 Hz), 119.36 (d, *J* = 8.0 Hz), 115.64 (d, *J* = 21 Hz), 113.16 (d, *J* = 2.0 Hz), 112.45, 109.60, 56.28.

4-Bromo-2-(3-fluorophenyl)benzo[*d*]oxazole (8e). According to the procedure A, **8e** was synthesized by intermolecular condensation reaction of 2-amino-3-bromophenol (1 mmol, 188 mg) and 3-fluorobenzoyl chloride (1 mmol, 158.5 mg) as a white solid (isolated yield = 58%). M. p.: 131.4–133.5 °C. ^{1}H NMR (400 MHz, $CDCl_3$) δ 8.09 (d, *J* = 7.8 Hz, 1H), 8.01–7.98 (m, 1H), 7.55–7.48 (m, 3H), 7.27–7.23 (m, 2H). ^{13}C NMR (101 MHz, $CDCl_3$) δ 162.87 (d, *J* = 246 Hz), 162.24 (d, *J* = 3.0 Hz), 150.84, 141.51, 130.64 (d, *J* = 8.0 Hz), 128.59 (d, *J* = 9.0 Hz), 128.02, 126.29, 123.70 (d, *J* = 3.0 Hz), 118.97 (d, *J* = 21 Hz), 114.88 (d, *J* = 24 Hz), 112.97, 109.84.

4-Bromo-2-(4-fluorophenyl)benzo[*d*]oxazole (8f). According to the procedure A, **8f** was synthesized by intermolecular condensation reaction of 2-amino-3-bromophenol (1 mmol, 188 mg) and 4-fluorobenzoyl chloride (1 mmol, 158.5 mg) as a white solid (isolated yield = 73%). M. p.: 137.4–138.2 °C. ^{1}H NMR (400 MHz, $CDCl_3$) δ 8.29 (dd, *J* = 8.8, 5.4 Hz, 2H), 7.52 (dd, *J* = 8.0, 2.6 Hz, 2H), 7.24–7.18 (m, 3H). ^{13}C NMR (101 MHz, $CDCl_3$) δ 165.06 (d, *J* = 252 Hz), 162.5, 150.81, 141.61, 130.25 (d, *J* = 9.0 Hz), 127.86, 125.91, 122.89 (d, *J* = 3.0 Hz), 116.19 (d, *J* = 22 Hz), 112.67, 109.70.

4-Bromo-2-(4-chlorophenyl)benzo[*d*]oxazole (8g). According to the procedure A, **8g** was synthesized by intermolecular condensation reaction of 2-amino-3-bromophenol (1 mmol, 188 mg) and 4-chlorobenzoyl chloride (1 mmol, 175 mg) as a white solid (isolated yield = 72%). M. p.: 172.9–174.1 °C. ^{1}H NMR (400 MHz, $CDCl_3$) δ 8.22 (d, *J* = 8.6 Hz, 2H), 7.54–7.49 (m, 4H), 7.23 (t, *J* = 8.0 Hz, 1H). ^{13}C NMR (101 MHz, $CDCl_3$) δ 162.49, 150.79, 141.56, 138.25, 129.25, 129.18, 127.94, 126.11, 125.04, 112.80, 109.75.

4-Bromo-2-(*p*-tolyl)benzo[*d*]oxazole (8h). According to the procedure A, **8h** was synthesized by intermolecular condensation reaction of 2-amino-3-bromophenol (1 mmol, 188 mg) and 4-methylbenzoyl chloride (1 mmol, 154 mg) as a white solid (isolated yield = 81%). M. p.: 102.7–103.6 °C. ^{1}H NMR (400 MHz, $CDCl_3$) δ 8.16 (d, *J* = 8.2 Hz, 2H), 7.48 (dd, *J* = 8.0, 1.4 Hz, 2H), 7.30 (d, *J* = 8.2 Hz, 2H), 7.18 (t, *J* = 8.0 Hz, 1H), 2.41 (s, 3H). ^{13}C NMR (101 MHz, $CDCl_3$) δ 163.68, 150.68, 142.50, 141.69, 129.54, 127.89, 127.60, 125.56, 123.74, 112.44, 109.56, 21.63.

4.1.2. General procedures for the synthesis of trimethoxyphenylbenzo[d]oxazoles 4a-u and 5a-h

To a mixture of bromobenzo[*d*]oxazoles (1 mmol) and K_2CO_3 (1.09 mmol, 0.15 g) in mixed solvent (DMF: EtOH: H_2O = 7:2:1, 5 mL), a solution of $Pd(PPh_3)_4$ (0.04 mmol, 0.046 g) in mixed solvent (DMF: EtOH: H_2O = 7:2:1, 0.5 mL) was added under Ar at 80 °C. Then, the reaction mixture was stirred at 80 °C for 10 h. After the reaction was completed, the reaction mixture was cool to room temperature, and dumped into the water (50 mL), and extracted with ethyl acetate (3 × 15 mL). The organic layer was dried by sodium sulfate and concentrated in a vacuum to provide a crude. The obtained crude was purified by chromatography (n-hexane: ethyl acetate = 10:1, v\v) to yield the corresponding trimethoxyphenylbenzo[*d*]oxazoles.

2-Phenyl-7-(3,4,5-trimethoxyphenyl)benzo[*d*]oxazole (4a). White solid (isolated yield = 79%). M. p.: 154.4–155.6 °C. ^{1}H NMR (400 MHz, $CDCl_3$) δ 8.27–8.25 (m, 2H), 7.75 (d, *J* = 7.8 Hz, 1H), 7.55–7.52 (m, 4H), 7.43 (t, *J* = 7.8 Hz, 1H), 7.15 (s, 2H), 3.99 (s, 6H), 3.96 (s, 3H). ^{13}C NMR (101 MHz, $CDCl_3$) δ 163.10, 153.51, 148.07,

142.81, 138.18, 131.66, 131.17, 129.01, 127.53, 127.09, 125.08, 123.96, 118.97, 105.58, 61.00, 56.28. HR-MS (ESI) calcd for $C_{22}H_{20}NO_4$ [M + H]$^+$: 362.1387, found: 362.1398.

2-(4-Methoxyphenyl)-7-(3,4,5-trimethoxyphenyl)benzo[*d*] oxazole (4b). White solid (isolated yield = 73%). M. p.: 136.5–137.4 °C. ^{1}H NMR (400 MHz, $CDCl_3$) δ 8.19 (d, *J* = 8.8 Hz, 2H), 7.70 (d, *J* = 7.8 Hz, 1H), 7.49 (d, *J* = 7.6 Hz, 1H), 7.40 (t, *J* = 7.8 Hz, 1H), 7.14 (s, 2H), 7.03 (d, *J* = 8.8 Hz, 2H), 3.99 (s, 6H), 3.96 (s, 3H), 3.89 (s, 3H). ^{13}C NMR (101 MHz, $CDCl_3$) δ 163.21, 162.41, 153.47, 147.94, 142.97, 138.10, 131.28, 129.27, 124.88, 124.82, 123.45, 119.55, 118.57, 114.44, 105.56, 60.98, 56.25, 55.44. HR-MS (ESI) calcd for $C_{23}H_{22}NO_5$[M + H]$^+$: 392.1493, found: 392.1507.

2-(3-Methoxyphenyl)-7-(3,4,5-trimethoxyphenyl)benzo[*d*] oxazole (4c). White solid (isolated yield = 67%). M. p.: 123.3–124.7 °C. ^{1}H NMR (400 MHz, $CDCl_3$) δ 7.85 (d, *J* = 7.6 Hz, 1H), 7.80 (s, 1H), 7.75 (d, *J* = 7.8 Hz, 1H), 7.53 (d, *J* = 7.8 Hz, 1H), 7.44 (t, *J* = 7.6 Hz, 2H), 7.16 (s, 2H), 7.11–7.09 (m, 1H), 3.99 (s, 6H), 3.96 (s, 3H), 3.91 (s, 3H). ^{13}C NMR (101 MHz, $CDCl_3$) δ 163.02, 160.00, 153.52, 148.06, 142.78, 138.16, 131.13, 130.10, 128.26, 125.10, 125.06, 123.99, 119.96, 118.97, 118.31, 112.00, 105.53, 61.01, 56.25, 55.49. HR-MS (ESI) calcd for $C_{23}H_{22}NO_5$ [M + H]$^+$: 392.1493, found: 392.1505.

2-(3,4-Dimethoxyphenyl)-7-(3,4,5-trimethoxyphenyl)benzo [*d*]oxazole (4d). Light pink solid (isolated yield = 47%). M. p.: 162.5–163.7 °C. ^{1}H NMR (400 MHz, $CDCl_3$) δ 7.84 (d, *J* = 8.4 Hz, 1H), 7.78 (s, 1H), 7.71 (d, *J* = 7.8 Hz, 1H), 7.50 (d, *J* = 7.6 Hz, 1H), 7.42 (t, *J* = 7.8 Hz, 1H), 7.16 (s, 2H), 7.00 (d, *J* = 8.4 Hz, 1H), 4.01 (s, 3H), 3.99 (s, 6H), 3.97 (s, 3H), 3.96 (s, 3H). ^{13}C NMR (101 MHz, $CDCl_3$) δ 163.21, 153.50, 152.14, 149.33, 148.00, 142.91, 138.12, 131.26, 124.99, 124.84, 123.57, 121.08, 119.67, 118.58, 111.09, 110.00, 105.55, 61.01, 56.24, 56.09, 56.06. HR-MS (ESI) calcd for $C_{24}H_{24}NO_6$ [M + H]$^+$: 422.1598, found: 422.1612.

2-(3-Fluoro-4-methoxyphenyl)-7-(3,4,5-trimethoxyphenyl) benzo[*d*]oxazole (4e). White solid (isolated yield = 51%). M. p.: 160.1–161.2 °C. ^{1}H NMR (400 MHz, $CDCl_3$) δ 8.01 (d, *J* = 8.6 Hz, 1H), 7.97–7.94 (m, 1H), 7.71 (d, *J* = 7.8 Hz, 1H), 7.51 (d, *J* = 7.6 Hz, 1H), 7.42 (t, *J* = 7.8 Hz, 1H), 7.12–7.07 (m, 3H), 3.99 (s, 6H), 3.98 (s, 3H), 3.96 (s, 3H). ^{13}C NMR (101 MHz, $CDCl_3$) δ 162.09 (d, *J* = 2.0 Hz), 153.53, 152.30 (d, *J* = 246 Hz), 150.70 (d, *J* = 11 Hz), 148.02, 142.82, 138.22, 131.14, 125.11, 125.01, 124.20 (d, *J* = 4.0 Hz), 123.88, 119.96 (d, *J* = 7.0 Hz), 118.78, 115.29 (d, *J* = 21 Hz), 113.37(d, *J* = 2.0 Hz), 105.59, 61.01, 56.32, 56.28. HR-MS (ESI) calcd for $C_{23}H_{21}NO_5F$ [M + H]$^+$: 410.1396, found: 410.1412.

2-(3-Fluorophenyl)-7-(3,4,5-trimethoxyphenyl)benzo[*d*]oxazole (4f). White solid (isolated yield = 54%). M. p.: 116.5–117.9 °C. ^{1}H NMR (400 MHz, $CDCl_3$) δ 8.05 (d, *J* = 7.8 Hz, 1H), 7.95 (d, *J* = 9.2 Hz, 1H), 7.75 (d, *J* = 7.8 Hz, 1H), 7.55 (d, *J* = 7.6 Hz, 1H), 7.52–7.49 (m, 1H), 7.45 (t, *J* = 7.8 Hz, 1H), 7.24–7.23 (m, 1H), 7.13 (s, 2H), 3.99 (s, 6H), 3.96 (s, 3H). ^{13}C NMR (101 MHz, $CDCl_3$) δ 162.93 (d, *J* = 246 Hz), 161.86 (d, *J* = 3.0 Hz), 153.55, 148.09, 142.65, 138.28, 130.99, 130.76 (d, *J* = 8.0 Hz), 129.13 (d, *J* = 9.0 Hz), 125.28, 125.26 (d, *J* = 4.0 Hz), 124.37, 123.21 (d, *J* = 3.0 Hz), 119.15, 118.65 (d, *J* = 22 Hz), 114.47 (d, *J* = 24 Hz), 105.59, 61.01, 56.28. HR-MS (ESI) calcd for $C_{22}H_{19}NO_4F$ [M + H]$^+$: 380.1293, found: 380.1304.

2-(4-Fluorophenyl)-7-(3,4,5-trimethoxyphenyl)benzo[*d*]oxazole (4g). White solid (isolated yield = 58%). M. p.: 148.5–149.7 °C. ^{1}H NMR (400 MHz, $CDCl_3$) δ 8.28–8.24 (m, 2H), 7.73 (d, *J* = 7.6 Hz, 1H), 7.52 (d, *J* = 7.2 Hz, 1H), 7.44 (t, *J* = 7.8 Hz, 1H), 7.23 (t, *J* = 8.6 Hz, 2H), 7.12 (s, 2H), 3.98 (s, 6H), 3.96 (s, 3H). ^{13}C NMR (101 MHz, $CDCl_3$) δ 164.87 (d, *J* = 252 Hz), 162.24, 153.53, 148.08, 142.72, 138.25, 131.12, 129.75 (d, *J* = 9.0 Hz), 125.17, 125.16 (d, *J* = 2.0 Hz), 124.08, 123.41 (d, *J* = 3.0 Hz), 118.92, 116.33 (d, *J* = 22 Hz), 105.63, 61.01, 56.30. HR-MS (ESI) calcd for $C_{22}H_{19}NO_4F$ [M + H]$^+$: 380.1293, found: 380.1290.

2-(3-Bromophenyl)-7-(3,4,5-trimethoxyphenyl)benzo[d] oxazole (4h). White solid (isolated yield = 62%). M. p.: 148.3–149.9 °C. ^{1}H NMR (400 MHz, $CDCl_3$) δ 8.42 (s, 1H), 8.19 (d, *J* = 7.8 Hz, 1H), 7.75 (d, *J* = 8.0 Hz, 1H), 7.68 (dd, *J* = 8.0, 0.8 Hz, 1H), 7.56 (d, *J* = 7.8 Hz, 1H), 7.47–7.40 (m, 2H), 7.14 (s, 2H), 4.00 (s, 6H), 3.96 (s, 3H). ^{13}C NMR (101 MHz, $CDCl_3$) δ 161.51, 153.56, 148.09, 142.64, 138.27, 134.51, 130.93, 130.58, 130.52, 128.99, 125.92, 125.33, 125.19, 124.33, 123.08, 119.17, 105.53, 61.03, 56.27. HR-MS (ESI) calcd for $C_{22}H_{19}NO_4Br$ [M + H]$^+$: 440.0492, found: 440.0511.

2-(4-Bromophenyl)-7-(3,4,5-trimethoxyphenyl)benzo[d] oxazole (4i). White solid (isolated yield = 61%). M. p.: 135.9–137.5 °C. ^{1}H NMR (400 MHz, $CDCl_3$) δ 8.19 (d, *J* = 8.4 Hz, 2H), 7.74 (d, *J* = 7.8 Hz, 1H), 7.54–7.50 (m, 3H), 7.44 (t, *J* = 7.8 Hz, 1H), 7.12 (s, 2H), 3.98 (s, 6H), 3.96 (s, 3H). ^{13}C NMR (101 MHz, $CDCl_3$) δ 162.13, 153.53, 148.07, 142.69, 138.26, 137.93, 131.05, 129.38, 128.73, 125.56, 125.23, 125.19, 124.25, 119.01, 105.61, 61.00, 56.28. HR-MS (ESI) calcd for $C_{22}H_{19}NO_4Br$ [M + H] + : 440.0492, found: 440.0609.

2-(3-Chlorophenyl)-7-(3,4,5-trimethoxyphenyl)benzo[d] oxazole (4j). White solid (isolated yield = 61%). M. p.: 145.6–147.5 °C. ^{1}H NMR (400 MHz, $CDCl_3$) δ 8.26 (s, 1H), 8.14 (d, *J* = 7.2 Hz, 1H), 7.75 (d, *J* = 7.8 Hz, 1H), 7.56–7.43 (m, 4H), 7.14 (s, 2H), 4.00 (s, 6H), 3.96 (s, 3H). ^{13}C NMR (101 MHz, $CDCl_3$) δ 161.68, 153.55, 148.09, 142.64, 138.26, 135.17, 131.60, 130.95, 130.35, 128.78, 127.60, 125.49, 125.32, 125.22, 124.35, 119.17, 105.53, 61.02, 56.27. HR-MS (ESI) calcd for $C_{22}H_{19}NO_4Cl$ [M + H]$^+$: 396.0997, found: 396.1011.

2-(4-Chlorophenyl)-7-(3,4,5-trimethoxyphenyl)benzo[*d*]oxazole (4k). White solid (isolated yield = 75%). M. p.: 144.0–145.1 °C. ^{1}H NMR (400 MHz, $CDCl_3$) δ 8.19 (d, *J* = 8.6 Hz, 2H), 7.74 (dd, *J* = 7.8, 1.2 Hz, 1H), 7.54–7.50 (m, 3H), 7.44 (t, *J* = 7.8 Hz, 1H), 7.12 (s, 2H), 3.98 (s, 6H), 3.96 (s, 3H). ^{13}C NMR (101 MHz, $CDCl_3$) δ 162.12, 153.54, 148.08, 142.72, 138.27, 137.91, 131.06, 129.38, 128.72, 125.58, 125.23, 125.18, 124.24, 119.02, 105.62, 61.00, 56.29. HR-MS (ESI) calcd for $C_{22}H_{19}NO_4Cl$ [M + H]$^+$: 396.0997, found: 396.1011.

2-(*p*-Tolyl)-7-(3,4,5-trimethoxyphenyl)benzo[d]oxazole (4l). Light pink solid (isolated yield = 86%). M. p.: 147.5–148.8 °C. ^{1}H NMR (400 MHz, $CDCl_3$) δ 8.15 (d, *J* = 8.0 Hz, 2H), 7.73 (d, *J* = 7.8 Hz, 1H), 7.51 (d, *J* = 7.2 Hz, 1H), 7.42 (t, *J* = 7.8 Hz, 1H), 7.34 (d, *J* = 8.0 Hz, 2H), 7.15 (s, 2H), 3.99 (s, 6H), 3.96 (s, 3H), 2.45 (s, 3H). ^{13}C NMR (101 MHz, $CDCl_3$) δ 163.36, 153.50, 147.99, 142.91, 142.24, 138.16, 131.24, 129.74, 127.50, 124.97, 124.95, 124.33, 123.71, 118.81, 105.59, 61.00, 56.27, 21.64. HR-MS (ESI) calcd for $C_{23}H_{22}NO_4$[M + H]$^+$: 376.1543, found: 376.1558.

2-(*m*-Tolyl)-7-(3,4,5-trimethoxyphenyl)benzo[*d*]oxazole (4m). White solid (isolated yield = 54%). M. p.: 152.9–154.2 °C. ^{1}H NMR (400 MHz, $CDCl_3$) δ 8.11 (s, 1H), 8.05 (d, *J* = 7.6 Hz, 1H), 7.74 (dd, *J* = 7.8, 1.0 Hz, 1H), 7.53 (dd, *J* = 7.8, 1.0 Hz, 1H), 7.45–7.41 (m, 2H), 7.36 (d, *J* = 7.4 Hz, 1H), 7.16 (s, 2H), 4.00 (s, 6H), 3.96 (s, 3H), 2.46 (s, 3H). ^{13}C NMR (101 MHz, $CDCl_3$) δ 163.28, 153.49, 148.02, 142.83, 138.82, 138.12, 132.48, 131.16, 128.91, 128.16, 126.92, 125.03, 124.97, 124.60, 123.81, 118.91, 105.51, 61.00, 56.22, 21.36. HR-MS (ESI) calcd for $C_{23}H_{22}NO_4$ [M + H]$^+$: 376.1543, found: 376.1555.

3-(7-(3,4,5-Trimethoxyphenyl)benzo[d]oxazol-2-yl)phenol (4n). The condensation reaction of **6b** and 4-hydroxybenzaldehyde give intermediate product **7n**, which was directly used without separation and purification in the next step for the synthesis of **4n** as white solid (isolated yield = 81%). M. p.: 244.4–245.4 °C. ^{1}H NMR (400 MHz, DMSO-d_6) δ 9.98 (s, 1H), 7.78 (d, *J* = 7.8 Hz, 1H), 7.72 (d, *J* = 7.6 Hz, 1H), 7.67 (d, *J* = 7.6 Hz, 1H), 7.61 (s, 1H), 7.49 (t, *J* = 7.8 Hz, 1H), 7.44 (t, *J* = 8.0 Hz, 1H), 7.26 (s, 2H), 7.03 (d, *J* = 7.8 Hz, 1H), 3.93 (s, 6H), 3.76 (s, 3H). ^{13}C NMR (101 MHz, DMSO-d_6) δ 162.63, 158.10, 153.39, 147.62, 142.46, 137.81, 130.77, 130.52, 127.69, 125.43, 124.62, 124.25, 119.37, 118.93, 118.23, 113.78, 105.66, 60.31, 56.21. HR-MS (ESI) calcd for $C_{22}H_{18}NO_5$ [M − H]$^-$: 376.1190, found: 376.1185.

2-Methoxy-4-(7-(3,4,5-trimethoxyphenyl)benzo[d]oxazol-2-yl)phenol (4o). The condensation reaction of **6b** and 4-hydroxy-3-methoxybenzaldehyde give intermediate product **7o**, which was directly used without separation and purification in the next step

for the synthesis of **4o** as white solid (isolated yield = 63%). M. p.: 120.6–121.5 °C. ^{1}H NMR (400 MHz, DMSO-d_6) δ 9.98 (s, 1H), 7.72–7.70 (m, 4H), 7.45 (t, J = 7.8 Hz, 1H), 7.30 (s, 2H), 7.01 (d, J = 8.8 Hz, 1H), 3.94 (s, 6H), 3.90 (s, 3H), 3.76 (s, 3H). ^{13}C NMR (101 MHz, DMSO-d_6) δ 163.06, 153.39, 150.72, 148.18, 147.51, 142.77, 137.77, 130.54, 125.26, 124.19, 123.53, 121.37, 118.42, 117.49, 116.27, 110.65, 105.55, 60.31, 56.16, 55.70. Negative HR-MS (ESI) calcd for $C_{23}H_{20}NO_6$ [M − H]$^-$: 406.1296, found: 406.1290.

4-(7-(3,4,5-Trimethoxyphenyl)benzo[d]oxazol-2-yl)aniline (4p). Light gray solid (isolated yield = 76%). M. p.: 203.5–204.2 °C. ^{1}H NMR (400 MHz, DMSO-d_6) δ 7.88 (d, J = 8.4 Hz, 2H), 7.62 (t, J = 8.4 Hz, 2H), 7.40 (t, J = 7.8 Hz, 1H), 7.25 (s, 2H), 6.71 (d, J = 8.4 Hz, 2H), 5.99 (s, 2H), 3.92 (s, 6H), 3.76 (s, 3H). ^{13}C NMR (101 MHz, DMSO-d_6) δ 163.88, 153.34, 152.75, 147.27, 143.08, 137.67, 130.79, 129.10, 124.95, 123.97, 122.89, 117.91, 113.79, 112.84, 105.56, 60.29, 56.16. HR-MS (ESI) calcd for $C_{22}H_{21}N_2O_4$ [M + H]$^+$: 377.1496, found: 377.1492.

3-(7-(3,4,5-Trimethoxyphenyl)benzo[d]oxazol-2-yl)aniline (4q). Light gray solid (isolated yield = 68%). M. p.: 165.8–167.1 °C. ^{1}H NMR (400 MHz, DMSO-d_6) δ 7.75 (d, J = 7.8 Hz, 1H), 7.70 (d, J = 7.6 Hz, 1H), 7.47 (t, J = 7.8 Hz, 1H), 7.44 (s, 1H), 7.36 (t, J = 8.2 Hz, 1H), 7.27–7.23 (m, 3H), 6.81 (d, J = 8.0 Hz, 1H), 5.50 (s, 2H), 3.93 (s, 6H), 3.76 (s, 3H). ^{13}C NMR (101 MHz, DMSO-d_6) δ 163.34, 153.37, 149.61, 147.54, 142.53, 137.74, 130.59, 129.99, 127.05, 125.31, 124.55, 124.07, 118.78, 117.52, 114.75, 112.11, 105.60, 60.29, 56.19. HR-MS (ESI) calcd for $C_{22}H_{21}N_2O_4$ [M + H]$^+$: 377.1496, found: 377.1493.

2-(1*H*-Indol-5-yl)-7-(3,4,5-trimethoxyphenyl)benzo[d]oxazole (4r). White solid (isolated yield = 82%). M. p.: 214.1–214.7 °C. ^{1}H NMR (400 MHz, DMSO-d_6) δ 11.53 (s, 1H), 8.48 (s, 1H), 7.99 (d, J = 8.4 Hz, 1H), 7.73 (d, J = 7.8 Hz, 1H), 7.68 (d, J = 7.6 Hz, 1H), 7.63 (d, J = 8.4 Hz, 1H), 7.51 (s, 1H), 7.46 (t, J = 7.8 Hz, 1H), 7.31 (s, 2H), 6.66 (s, 1H), 3.96 (s, 6H), 3.78 (s, 3H). ^{13}C NMR (101 MHz, DMSO-d_6) δ 164.45, 153.40, 147.59, 142.95, 138.03, 137.77, 130.74, 128.01, 127.53, 125.17, 124.28, 123.45, 120.46, 120.45, 118.40, 117.39, 112.55, 105.66, 102.68, 60.34, 56.21. Negative HR-MS (ESI) calcd for $C_{24}H_{19}N_2O_4$ [M − H]$^-$: 399.1350, found: 399.1344.

2-(1*H*-Indol-5-yl)-7-(2,3,4-trimethoxyphenyl)benzo[*d*]oxazole (4s). White solid (isolated yield = 76%). M. p.: 116.6–167.8 °C. ^{1}H NMR (400 MHz, DMSO-d_6) δ 11.49 (s, 1H), 8.38 (s, 1H), 7.92 (d, J = 9.0 Hz, 1H), 7.71 (d, J = 7.8 Hz, 1H), 7.57 (d, J = 8.6 Hz, 1H), 7.48 (s, 1H), 7.41 (t, J = 7.8 Hz, 1H), 7.33 (d, J = 7.6 Hz, 1H), 7.27 (d, J = 8.6 Hz, 1H), 7.00 (d, J = 8.6 Hz, 1H), 6.62 (s, 1H), 3.90 (s, 3H), 3.85 (s, 3H), 3.74 (s, 3H). ^{13}C NMR (101 MHz, DMSO-d_6) δ 164.21, 153.97, 151.45, 148.35, 142.18, 142.06, 137.94, 127.93, 127.44, 125.69, 125.43, 124.59, 121.94, 120.48, 120.37, 118.05, 117.39, 112.44, 108.20, 102.61, 61.10, 60.61, 56.14. HR-MS (ESI) calcd for $C_{24}H_{21}N_2O_4$ [M + H]$^+$: 401.1496, found: 401.1494.

2-(Furan-2-yl)-7-(3,4,5-trimethoxyphenyl)benzo[d]oxazole (4t). light pink solid (isolated yield = 65%). M. p.: 144.2–145.7 °C. ^{1}H NMR (400 MHz, $CDCl_3$) δ 7.72 (d, J = 7.8 Hz, 1H), 7.68 (d, J = 0.8 Hz, 1H), 7.53 (d, J = 7.2 Hz, 1H), 7.43 (t, J = 7.8 Hz, 1H), 7.27 (s, 1H), 7.12 (s, 2H), 6.64–6.62 (m, 1H), 3.98 (s, 6H), 3.94 (s, 3H). ^{13}C NMR (101 MHz, $CDCl_3$) δ 155.39, 153.49, 147.46, 145.86, 142.54, 142.35, 138.20, 130.88, 125.30, 125.06, 124.06, 119.02, 114.30, 112.26, 105.56, 60.97, 56.23. HRMS (ESI) calcd for $C_{20}H_{18}NO_5$ [M + H]$^+$: 352.1180, found: 352.1190.

2-(Thiophen-2-yl)-7-(3,4,5-trimethoxyphenyl)benzo[d]oxazole (4u). light pink solid (isolated yield = 53%). M. p.: 151.5–152.4 °C. ^{1}H NMR (400 MHz, $CDCl_3$) δ 7.91 (d, J = 3.6 Hz, 1H), 7.70 (d, J = 7.8 Hz, 1H), 7.57 (d, J = 4.8 Hz, 1H), 7.52 (d, J = 7.6 Hz, 1H), 7.42 (t, J = 7.8 Hz, 1H), 7.20 (t, J = 4.4 Hz, 1H), 7.15 (s, 2H), 3.99 (s, 6H), 3.95 (s, 3H). ^{13}C NMR (101 MHz, $CDCl_3$) δ 159.07, 153.47, 147.66, 142.72, 138.09, 130.92, 130.36, 129.87, 129.51, 128.36, 125.21, 124.78, 123.78, 118.71, 105.40, 60.98, 56.21. HRMS (ESI) calcd for $C_{20}H_{18}NO_4S$ [M + H]$^+$: 368.0951, found: 368.0960.

2-Phenyl-4-(3,4,5-trimethoxyphenyl)benzo[*d*]oxazole (5a). White solid (isolated yield = 71%). M. p.: 94.1–95.2 °C. ^{1}H NMR (400 MHz, $CDCl_3$) δ 8.30–8.28 (m, 2H), 7.56–7.52 (m, 5H), 7.41 (t, J = 7.8 Hz, 1H), 7.36 (s, 2H), 4.00 (s, 6H), 3.94 (s, 3H). ^{13}C NMR (101 MHz, $CDCl_3$) δ 162.82, 153.27, 151.40, 139.78, 138.06, 132.80, 132.68, 131.49, 128.85, 127.65, 127.20, 125.11, 123.04, 109.34, 106.37, 60.93, 56.24. HR-MS (ESI) calcd for $C_{22}H_{20}NO_4$ [M + H]$^+$: 362.1387, found: 362.1385.

2-(3,4-Dimethoxyphenyl)-4-(3,4,5-trimethoxyphenyl)benzo[*d*]oxazole (5b). White solid (isolated yield = 72%). M. p.: 107.9–109.1 °C. ^{1}H NMR (400 MHz, $CDCl_3$) δ 7.89 (dd, J = 8.4, 1.5 Hz, 1H), 7.80 (s, 1H), 7.54 (d, J = 4.0 Hz, 1H), 7.52 (d, J = 4.0 Hz, 1H), 7.38 (t, J = 8.0 Hz, 1H), 7.35 (s, 2H), 7.00 (d, J = 8.4 Hz, 1H), 4.00 (s, 3H), 3.99 (s, 6H), 3.97 (s, 3H), 3.94 (s, 3H). ^{13}C NMR (101 MHz, $CDCl_3$) δ 162.92, 153.25, 151.99, 151.35, 149.14, 139.93, 138.00, 132.78, 132.43, 124.68, 122.97, 121.27, 119.82, 111.05, 110.21, 109.15, 106.36, 60.93, 56.16, 56.03, 56.02. HR-MS (ESI) calcd for $C_{24}H_{24}NO_6$ [M + H]$^+$: 422.1598, found: 422.1595.

2-(3,5-Dimethoxyphenyl)-4-(3,4,5-trimethoxyphenyl)benzo[d]oxazole (5c): White solid (isolated yield = 64%). M. p.: 112.1–113.5 °C. ^{1}H NMR (400 MHz, $CDCl_3$) δ 7.55 (d, J = 3.2 Hz, 1H), 7.53 (d, J = 2.7 Hz, 1H), 7.44 (d, J = 2.2 Hz, 2H), 7.41 (t, J = 8.0 Hz, 1H), 7.35 (s, 2H), 6.63 (s, 1H), 3.99 (s, 6H), 3.94 (s, 3H), 3.88 (s, 6H). ^{13}C NMR (101 MHz, $CDCl_3$) δ 162.68, 161.03, 153.26, 151.36, 139.68, 138.05, 132.80, 132.62, 128.78, 125.21, 123.06, 109.35, 106.37, 105.40, 104.32, 60.93, 56.16, 55.56. HR-MS (ESI) calcd for $C_{24}H_{24}NO_6$ [M + H]$^+$: 422.1598, found: 422.1593.

2-(3-Fluoro-4-methoxyphenyl)-4-(3,4,5-trimethoxyphenyl)benzo[*d*]oxazole (5d). White solid (isolated yield = 64%). M. p.: 141.3–142.5 °C. ^{1}H NMR (400 MHz, $CDCl_3$) δ 8.04 (d, J = 8.8 Hz, 1H), 7.99 (dd, J = 11.7,1.8 Hz, 1H), 7.53 (d, J = 8.0 Hz, 2H), 7.40 (t, J = 8.4 Hz, 1H), 7.33 (s, 2H), 7.09 (t, J = 8.4 Hz, 1H), 3.99 (s, 6H), 3.98 (s, 3H), 3.94 (s, 3H). ^{13}C NMR (101 MHz, $CDCl_3$) δ 161.84 (d, J = 2.0 Hz), 153.28, 152.25 (d, J = 245 Hz), 151.36, 150.57 (d, J = 11 Hz), 139.79, 138.08, 132.67 (d, J = 2.0 Hz), 125.00, 124.34 (d, J = 3.0 Hz), 123.13, 120.13 (d, J = 7.0 Hz), 115.40 (d, J = 21 Hz), 113.24 (d, J = 2.0 Hz), 109.24, 106.36, 60.94, 56.31, 56.25. HR-MS (ESI) calcd for $C_{23}H_{21}NO_5F$ [M + H]$^+$: 410.1398, found: 410.1393.

2-(3-Fluorophenyl)-4-(3,4,5-trimethoxyphenyl)benzo[*d*]oxazole (5e): White solid (isolated yield = 61%). M. p.: 116.1–117.1 °C. ^{1}H NMR (400 MHz, $CDCl_3$) δ 8.08 (d, J = 7.8 Hz, 1H), 7.97 (d, J = 9.0 Hz, 1H), 7.57–7.53 (m, 2H), 7.51–7.48 (m, 1H), 7.44 (t, J = 8.0 Hz, 1H), 7.33 (s, 2H), 7.23 (dd, J = 8.4, 1.8 Hz, 1H), 3.99 (s, 6H), 3.94 (s, 3H). ^{13}C NMR (101 MHz, $CDCl_3$) δ 162.86 (d, J = 251 Hz), 161.65 (d, J = 3.0 Hz), 153.31, 151.42, 139.61, 138.16, 133.11, 132.51, 130.60 (d, J = 8.0 Hz), 129.24 (d, J = 9.0 Hz), 125.54, 123.37 (d, J = 3.0 Hz), 123.29, 118.50 (d, J = 21 Hz), 114.56 (d, J = 24 Hz), 109.43, 106.39, 60.95, 56.26. HR-MS (ESI) calcd for $C_{22}H_{19}NO_4F$ [M + H]$^+$: 380.1293, found: 380.1291.

2-(4-Fluorophenyl)-4-(3,4,5-trimethoxyphenyl)benzo[d]oxazole (5f): White solid(isolated yield = 67%). M. p.: 131.7–133.3 °C. ^{1}H NMR (400 MHz, $CDCl_3$) δ 8.29–8.26 (m, 2H), 7.54 (s, 1H), 7.52 (s, 1H), 7.41 (t, J = 8.0 Hz, 1H), 7.33 (s, 2H), 7.21 (t, J = 8.6 Hz, 2H), 3.99 (s, 6H), 3.94 (s, 3H). ^{13}C NMR (101 MHz, $CDCl_3$) δ 164.79 (d, J = 251 Hz), 161.94, 153.27, 151.38, 139.70, 138.09, 132.83, 132.61, 129.84 (d, J = 9.0 Hz), 125.13, 123.50 (d, J = 3.0 Hz), 123.16, 116.12 (d, J = 22 Hz), 109.29, 106.36, 60.92, 56.23. HR-MS (ESI) calcd for $C_{22}H_{19}NO_4F$ [M + H]$^+$: 380.1293, found: 380.1292.

2-(4-Chlorophenyl)-4-(3,4,5-trimethoxyphenyl)benzo[d]oxazole (5g). White solid (isolated yield = 69%). M. p.: 143.7–144.9 °C. ^{1}H NMR (400 MHz, $CDCl_3$) δ 8.21 (d, J = 8.4 Hz, 2H), 7.54 (d, J = 7.8 Hz, 2H), 7.50 (d, J = 8.4 Hz, 2H), 7.42 (t, J = 8.0 Hz, 1H), 7.32 (s, 2H), 3.99 (s, 6H), 3.94 (s, 3H). ^{13}C NMR (101 MHz, $CDCl_3$) δ 161.87, 153.29, 151.39, 139.68, 138.14, 137.74, 132.98, 132.56, 129.23, 128.88, 125.68, 125.36, 123.25, 109.35, 106.39, 60.94, 56.25.

HR-MS (ESI) calcd for $C_{22}H_{19}NO_4Cl$ $[M + H]^+$:396.0997, found: 396.0994.

2-(*p*-Tolyl)-4-(3,4,5-trimethoxyphenyl)benzo[d]oxazole (5h). White solid (isolated yield = 73%). M. p.: 113.3–114.5 °C. ^{1}H NMR (400 MHz, $CDCl_3$) δ 8.17 (d, J = 8.0 Hz, 2H), 7.54 (d, J = 2.6 Hz, 1H), 7.52 (d, J = 2.2 Hz, 1H), 7.39 (t, J = 7.8 Hz, 1H), 7.36 (s, 2H), 7.33 (d, J = 8.0 Hz, 2H), 3.99 (s, 6H), 3.94 (s, 3H), 2.44 (s, 3H). ^{13}C NMR (101 MHz, $CDCl_3$) δ 163.08, 153.26, 151.32, 142.03, 139.86, 138.01, 132.76, 132.61, 129.58, 127.63, 124.85, 124.43, 122.96, 109.24, 106.37, 60.93, 56.23, 21.65. HR-MS (ESI) calcd for $C_{23}H_{22}NO_4$ $[M + H]^+$: 376.1543, found: 376.1541.

4.2. Pharmacology

Cell culture, anti-proliferative assays, tubulin polymerization assay, inhibitory screening assay, and immunofluorescence staining of tubulin were performed according to our previously reported procedures [23–25,36–38], which are described in the Supporting Information.

4.2.1. Western blot assay

A549 cells were seeded into six-well plates and incubated overnight, then treated with 4r for 24 h at different concentrations (50, 100, and 500 nM). After the treatment, cells were lysed, and total protein was extracted in RIPA lysis buffer containing 1% protease inhibitors and 1% phosphatase inhibitors. Lysates were centrifuged for 15 min at 12,000 rpm, and the supernatants in a centrifuge tube were used for Western blot analysis. Proteins were separated by 10% SDS-PAGE and transferred to PVDF membranes. The membranes were blocked with 5% skim milk for 1 h at room temperature and then incubated overnight at 4 °C with the primary antibodies. On the next day, the membranes were washed three times with TBST (5 min each time) and then incubated with goat anti-mouse or anti-rabbit HRP-conjugated secondary antibody. Finally, the protein bands were visualized using an ECL Western Blot Kit and analyzed by the Image J software.

4.3. Molecular docking

Molecular docking was performed according to our previously reported procedures [23,29], which are described in the Supporting Information. The crystal structures tubulin with colchicine (PDB: 1SA0) [35] and PDE4D with roflumilast (PDB code 3G4L) [27] were used as the template.

Declaration of competing interest

The authors declare that they have no known competing financial interests or personal relationships that could have appeared to influence the work reported in this paper.

Acknowledgments

This work was financially supported by Foundation for National Natural Science Foundation of China (No. 81872735), and Guangdong Basic and Applied Basic Research Foundation (2018A030313046), and Guangzhou Science and Technology Plan Project (202102080483).

Appendix A. Supplementary data

Supplementary data to this article can be found online at https://doi.org/10.1016/j.ejmech.2021.113700.

References

[1] M.G. Savelieff, G. Nam, J. Kang, H.J. Lee, M. Lee, M.H. Lim, Development of multifunctional molecules as potential therapeutic candidates for Alzheimer's Disease, Parkinson's disease, and amyotrophic lateral sclerosis in the last decade, Chem. Rev. 119 (2019) 1221–1322.
[2] M. Yumura, T. Nagano, Y. Nishimura, Novel multitarget therapies for lung cancer and respiratory disease, Molecules 25 (2020) 3987.
[3] R. Ahmadi, M.A. Ebrahimzadeh, Resveratrol - a comprehensive review of recent advances in anticancer drug design and development, Eur. J. Med. Chem. 200 (2020) 112356.
[4] R.G. Kenny, C.J. Marmion, Toward multi-targeted platinum and ruthenium drugs-A new paradigm in cancer drug treatment regimens? Chem. Rev. 119 (2019) 1058–1137.
[5] S. Choudhary, P.K. Singh, H. Verma, H. Singh, O. Silakari, Success stories of natural product-based hybrid molecules for multi-factorial diseases, Eur. J. Med. Chem. 151 (2018) 62–97.
[6] X. Liang, P. Wu, Q. Yang, Y. Xie, C. He, L. Yin, Z. Yin, G. Yue, Y. Zou, L. Li, X. Song, C. Lv, W. Zhang, B. Jing, An update of new small-molecule anticancer drugs approved from 2015 to 2020, Eur. J. Med. Chem. 220 (2021) 113473.
[7] Z.T. Al-Salama, S.J. Keam, Entrectinib: first global approval, Drugs 79 (2019) 1477–1483.
[8] J. Dai, Y. Chen, C. Tang, X. Wei, Y. Gong, J. Wei, D. Gu, J. Chen, Pyrotinib in the treatment of human epidermal growth factor receptor 2-positive metastatic breast cancer: a case report, Medicine 99 (2020), e20809.
[9] D.A. Rodrigues, F.S. Sagrillo, C.A.M. Fraga, Duvelisib: a 2018 Novel FDA-approved small molecule inhibiting phosphoinositide 3-kinases, Pharmaceuticals (2019) 12, https://doi.org/10.3390/ph12020069.
[10] M. Massimi, F. Ragusa, S. Cardarelli, M. Giorgi, Targeting cyclic AMP signalling in hepatocellular carcinoma, Cells (2019) 8, https://doi.org/10.3390/cells8121511.
[11] D.J.P. Henderson, A. Byrne, G.S. Baillie, K. Dulla, R. Hoffmann, G. Jenster, M.D. Houslay, The cAMP phosphodiesterase-4D7 (PDE4D7) is downregulated in androgen-independent prostate cancer cells and mediates proliferation by compartmentalising cAMP at the plasma membrane of VCaP prostate cancer cells, Br. J. Canc. 110 (2014) 1278–1287.
[12] D.U. Kim, B. Kwak, S.-W. Kim, Phosphodiesterase 4B is an effective therapeutic target in colorectal cancer, Biochem. Biophys. Res. Commun. 508 (2019) 825–831.
[13] T. Peng, J. Gong, Y. Jin, Y. Zhou, R. Tong, X. Wei, L. Bai, J. Shi, Inhibitors of phosphodiesterase as cancer therapeutics, Eur. J. Med. Chem. 150 (2018) 742–756.
[14] S. Hsien Lai, G. Zervoudakis, J. Chou, M.E. Gurney, K.M. Quesnelle, PDE4 subtypes in cancer, Oncogene 39 (2020) 3791–3802.
[15] T. Peng, B. Qi, J. He, H. Ke, J. Shi, Advances in the development of phosphodiesterase-4 inhibitors, J. Med. Chem. 63 (2020) 10594–10617.
[16] Z. Chu, Q. Xu, Q. Zhu, X. Ma, J. Mo, G. Lin, Y. Zhao, Y. Gu, L. Bian, L. Shao, J. Guo, W. Ye, J. Li, G. He, Y. Xu, Design, synthesis and biological evaluation of novel benzoxaborole derivatives as potent PDE4 inhibitors for topical treatment of atopic dermatitis, Eur. J. Med. Chem. 213 (2021) 113171.
[17] Y. Lin, W. Ahmed, M. He, X. Xiang, R. Tang, Z.-N. Cui, Synthesis and bioactivity of phenyl substituted furan and oxazole carboxylic acid derivatives as potential PDE4 inhibitors, Eur. J. Med. Chem. 207 (2020) 112795.
[18] J. Liang, Y.-Y. Huang, Q. Zhou, Y. Gao, Z. Li, D. Wu, S. Yu, L. Guo, Z. Chen, L. Huang, S.H. Liang, X. He, R. Wu, H.-B. Luo, Discovery and optimization of α-mangostin derivatives as novel PDE4 Inhibitors for the treatment of vascular dementia, J. Med. Chem. 63 (2020) 3370–3380.
[19] R. Zhang, H. Li, X. Zhang, J. Li, H. Su, Q. Lu, G. Dong, H. Dou, C. Fan, Z. Gu, Q. Mu, W. Tang, Y. Xu, H. Liu, Design, synthesis, and biological evaluation of tetrahydroisoquinolines derivatives as novel, selective PDE4 inhibitors for antipsoriasis treatment, Eur. J. Med. Chem. 211 (2021) 113004.
[20] A.D. Tangutur, D. Kumar, K.V. Krishna, S. Kantevari, Microtubule targeting agents as cancer chemotherapeutics: an overview of molecular hybrids as stabilising and destabilising agents, Curr. Top. Med. Chem. 17 (2017) 2523–2537.
[21] L.R.P. de Siqueira, P.A.T. de Moraes Gomes, L.P. de Lima Ferreira, M.J.B. de Melo Rêgo, A.C.L. Leite, Multi-target compounds acting in cancer progression: focus on thiosemicarbazone, thiazole and thiazolidinone analogues, Eur. J. Med. Chem. 170 (2019) 237–260.
[22] A. Virgilio, D. Spano, V. Esposito, V. Di Dato, G. Citarella, N. Marino, V. Maffia, D. De Martino, P. De Antonellis, A. Galeone, M. Zollo, Novel pyrimidopyrimidine derivatives for inhibition of cellular proliferation and motility induced by h-prune in breast cancer, Eur. J. Med. Chem. 57 (2012) 41–50.
[23] J. He, M. Zhang, L. Tang, J. liu, J. Zhong, W. Wang, J.-P. Xu, H.-T. Wang, X.-F. Li, Z.-Z. Zhou, Synthesis, biological evaluation, and molecular docking of arylpyridines as antiproliferative agent targeting tubulin, ACS Med. Chem. Lett. 11 (2020) 1611–1619.
[24] Z.-Z. Zhou, X.-D. Shi, H.-F. Feng, Y.-F. Cheng, H.-T. Wang, J.-P. Xu, Discovery of 9H-purins as potential tubulin polymerization inhibitors: synthesis, biological evaluation and structure–activity relationships, Eur. J. Med. Chem. 138 (2017) 1126–1134.
[25] B.-C. Ge, H.-F. Feng, Y.-F. Cheng, H.-T. Wang, B.-M. Xi, X.-M. Yang, J.-P. Xu, Z.-Z. Zhou, Design, synthesis and biological evaluation of substituted aminopyridazin-3(2H)-ones as G0/G1-phase arresting agents with apoptosis-

inducing activities, Eur. J. Med. Chem. 141 (2017) 440–445.
[26] G.-H. Yan, X.-F. Li, B.-C. Ge, X.-D. Shi, Y.-F. Chen, X.-M. Yang, J.-P. Xu, S.-W. Liu, P.-L. Zhao, Z.-Z. Zhou, C.-Q. Zhou, W.-H. Chen, Synthesis and anticancer activities of 3-arylflavone-8-acetic acid derivatives, Eur. J. Med. Chem. 90 (2015) 251–257.
[27] A.B. Burgin, O.T. Magnusson, J. Singh, P. Witte, B.L. Staker, J.M. Bjornsson, M. Thorsteinsdottir, S. Hrafnsdottir, T. Hagen, A.S. Kiselyov, L.J. Stewart, M.E. Gurney, Design of phosphodiesterase 4D (PDE4D) allosteric modulators for enhancing cognition with improved safety, Nat. Biotechnol. 28 (2010) 63–70.
[28] R. Aspiotis, D. Deschenes, D. Dube, Y. Girard, Z. Huang, F. Laliberte, S. Liu, R. Papp, D.W. Nicholson, R.N. Young, The discovery and synthesis of highly potent subtype selective phosphodiesterase 4D inhibitors, Bioorg. Med. Chem. Lett 20 (2010) 5502–5505.
[29] L. Tang, C. Huang, J. Zhong, J. He, J. Guo, M. Liu, J.-P. Xu, H.-T. Wang, Z.-Z. Zhou, Discovery of arylbenzylamines as PDE4 inhibitors with potential neuroprotective effect, Eur. J. Med. Chem. 168 (2019) 221–231.
[30] T. Tsunoda, T. Ota, T. Fujimoto, K. Doi, Y. Tanaka, Y. Yoshida, M. Ogawa, H. Matsuzaki, M. Hamabashiri, D.R. Tyson, M. Kuroki, S. Miyamoto, S. Shirasawa, Inhibition of phosphodiesterase-4 (PDE4) activity triggers luminal apoptosis and AKT dephosphorylation in a 3-D colonic-crypt model, Mol. Canc. 11 (2012) 46.
[31] L.Y. Xia, Y.L. Zhang, R. Yang, Z.C. Wang, Y.D. Lu, B.Z. Wang, H.L. Zhu, Tubulin inhibitors binding to colchicine-site: a Review from 2015 to 2019, Curr. Med. Chem. 26 (2019) 1–27.
[32] L. Li, S. Jiang, X. Li, Y. Liu, J. Su, J. Chen, Recent advances in trimethoxyphenyl (TMP) based tubulin inhibitors targeting the colchicine binding site, Eur. J. Med. Chem. 151 (2018) 482–494.
[33] M. Massimi, S. Cardarelli, F. Galli, M.F. Giardi, F. Ragusa, N. Panera, B. Cinque, M.G. Cifone, S. Biagioni, M. Giorgi, Increase of intracellular cyclic AMP by PDE4 inhibitors affects HepG2 cell cycle progression and survival, J. Cell. Biochem. 118 (2017) 1401–1411.
[34] T.C. Chen, P. Wadsten, S. Su, N. Rawlinson, F.M. Hofman, C.K. Hill, A.H. Schonthal, The type IV phosphodiesterase inhibitor rolipram induces expression of the cell cycle inhibitors p21(Cip1) and p27(Kip1), resulting in growth inhibition, increased differentiation, and subsequent apoptosis of malignant A-172 glioma cells, Canc. Biol. Ther. 1 (2002) 268–276.
[35] R.B. Ravelli, B. Gigant, P.A. Curmi, I. Jourdain, S. Lachkar, A. Sobel, M. Knossow, Insight into tubulin regulation from a complex with colchicine and a stathmin-like domain, Nature 428 (2004) 198–202.
[36] Z.-Z. Zhou, B.-C. Ge, Q.-P. Zhong, C. Huang, Y.-F. Cheng, X.-M. Yang, H.-T. Wang, J.-P. Xu, Development of highly potent phosphodiesterase 4 inhibitors with anti-neuroinflammation potential: design, synthesis, and structure-activity relationship study of catecholamides bearing aromatic rings, Eur. J. Med. Chem. 124 (2016) 372–379.
[37] Z.-Z. Zhou, Y.-F. Cheng, Z.-Q. Zou, B.-C. Ge, H. Yu, C. Huang, H.-T. Wang, X.-M. Yang, J.-P. Xu, Discovery of N-alkyl catecholamides as selective phosphodiesterase-4 Inhibitors with anti-neuroinflammation potential Exhibiting antidepressant-like effects at non-emetic Doses, ACS Chem. Neurosci. 8 (2017) 135–146.
[38] Z.-Z. Zhou, B.-C. Ge, Y.-F. Chen, X.-D. Shi, X.-M. Yang, J.-P. Xu, Catecholic amides as potential selective phosphodiesterase 4D inhibitors: design, synthesis, pharmacological evaluation and structure–activity relationships, Bioorg. Med. Chem. 23 (2015) 7332–7339.